THESIS FOR THE DEGREE OF LICENTIATE OF ENGINEERING

Technical Report No. 340L

On feature extraction of voltage disturbance signals

EMMANOUIL STYVAKTAKIS

Department of Signals and Systems
School of Electrical and Computer Engineering
CHALMERS UNIVERSITY OF TECHNOLOGY
S-412 96 Göteborg, Sweden
March 2000

On feature extraction of voltage disturbance signals
Technical Report No. 340L

Emmanouil Styvaktakis

Department of Signals and Systems
Chalmers University of Technology
S-412 96 Göteborg, Sweden

Tel. +46 31 772 1000, Fax. +46 31 772 1782
http://www.s2.chalmers.se

Printed by Chalmers Reproservice, Göteborg, March 2000.

ΠΑΝΤΩΝ ΧΡΗΜΑΤΩΝ ΜΕΤΡΟΝ ΑΝΘΡΩΠΟΣ
(Man is the measure of all things)

Πρωταγόρας

Abstract

Power quality, a recently introduced term, covers several phenomena related to the fact that voltage and current in an electric power system deviate from an ideal sinusoidal signal. The increased requirements on supervision, control, and performance in modern power systems make power quality monitoring necessary. However, the databases created by monitoring, are large and new tools are required for the fast and efficient use of the data.

This thesis focuses on a number of events that occur during power system operation and presents the results of the analysis of actual recordings. New classes of events are defined and the distinctive characteristics (features) of each class are given. The guidelines for the development of a knowledge-based classification system, which utilises these features, are given.

Two groups of power system events are considered in this thesis. The first group contains transients due to synchronised capacitor switching. An algorithm is proposed for the detection and classification of two types of synchronised switching. The second group contains events whose main characteristic is a temporary decrease in voltage (voltage dips). Several types are identified in this group. The distinctive characteristics of each type are also identified. Using these features, a large number of recordings from a medium voltage network are classified. The results show that new types of voltage dips must be considered when interpreting power quality monitoring data.

An interesting new type of power system event that was observed during a monitoring program is reported in detail. It was found that transformer saturation occurs due to voltage recovery after a voltage dip. This type of event has not been presented before in the literature.

Additionally, a new fault location technique for two and three terminal lines is presented. The technique utilises the high frequency fault-clearing transients of the voltage measured on the line side of the circuit breaker.

Keywords: power quality, power system monitoring, capacitor switching, voltage dips, power system faults, induction motors, transformer saturation, fault location, spectrum estimation. short time Fourier transform.

Acknowledgements

First, I would to thank my supervisor, Dr. Math Bollen, for all the help he offered me and for being a source of ideas and inspiration. Working with Math has been an experience which made my journey to Sweden a worthwhile one. Extra thanks for helping me with the manuscript.

I would like also to thank my second supervisor, Dr. Irene Gu for her help in signal processing, for interesting discussions and for her constant encouragement.

Thanks also goes to my examiner, Professor Mats Viberg for his careful proof-reading of this manuscript and for making the Signal Processing Group an excellent working environment. I am also thankful to Professor Jaap Daalder for always giving me useful comments. Many thanks to all the people in the Signal Processing Group for helping me in different ways and to Maxime Flament for helping me with my computer.

The research presented in this thesis has been funded through the Elektra program, which is jointly financed by Energimyndigheten, ABB Corporate Research and ABB Automation Products AB. The financial support is gratefully acknowledged. This project is a collaborated research between the Signal Processing group of the department of Signals and Systems and the department of Power Engineering at Chalmers University of Technology.

The work presented is highly related to measurements. I would like to thank all the power companies, which have supplied me with data: Scottish Power, Göteborg Energi Nät AB and SINTEF Energy Research. Special thanks goes to Alastair Ferguson from Scottish Power, Christian Roxenius and Robert Olofsson from Göteborg Energi Nät AB.

Finally, I would like to thank the members of the steering group of this project for contributing in very useful meetings and commenting on this thesis: Murari Mohan Saha from ABB Automation Products AB, Helge Seljeseth from SINTEF Energy Research, Magnus Olofsson from STRI AB, and Christian Roxenius from Göteborg Energi Nät AB.

List of publications

A E. Styvaktakis, M.H.J. Bollen, I.Y.H. Gu: A fault location technique using high frequency fault clearing transients, IEEE Power Engineering Letters, May 1999, pp. 58-60.

B E. Styvaktakis, M.H.J. Bollen, I.Y.H. Gu: A fault location technique for two and three-terminal lines using high frequency fault clearing transients, Budapest Power Tech '99, 29 Sep. -3 Aug. 1999.

C E. Styvaktakis, M.H.J. Bollen, I.Y.H. Gu: Classification of Power System Transients: Synchronised Switching, IEEE Winter Meeting, Singapore, 23-27 January 2000.

D E. Styvaktakis, M.H.J. Bollen, I.Y.H. Gu: Transformer saturation after a voltage dip. Submitted to IEEE Power Engineering Letters.

E E. Styvaktakis, M.H.J. Bollen, I.Y.H. Gu: Classification of power system events: Voltage dips. Submitted to the 9th International IEEE Conference on Harmonics and Quality of Power, October 1-4, 2000, Orlando, Florida USA.

Contents

Chapter 1 Introduction

1.1 Background

The increasing use of technology that is sensitive to power system disturbances, the increasing awareness of power quality issues and deregulation have created a need for extensive monitoring of the power system operation. Customers with sensitive equipment like adjustable speed drives, power electronics or computers expect by monitoring to locate the source of the problems that might occur. On the other side, utilities try to meet the demands of their customers. They monitor to prove that the quality of the offered power is within pre-specified standards and to find all the necessary information that will allow them to correct any problems. Finally, deregulation creates a challenging and competitive environment, where power quality could become a commodity (for example by offering different levels of guarantee to different customers) and as such it must be monitored and measured.

1.2 Motivation

The increased requirements of supervising in modern power systems make monitoring a necessary tool. The new advances in electronics and communications offer new options in monitoring large systems in an efficient and low cost way. Utilities can collect data from different parts of their networks, evaluate the performance of their protection systems, and respond fast to complains rising from the customer's side. Therefore, the installation of monitors is increasing and it is expected that in the following years more monitors will be employed.

Each monitoring program has its own targets and the monitors are set accordingly. Long sequences of data are captured by the monitors and they either contain events which need to be registered or events which are due to normal system operation which are not of particular interest and must be discarded. The databases, which are created, are large and difficult to be utilised efficiently. Automatic processing of the data is therefore necessary for fast and effective use of these databases.

Classification of the different power system events is necessary for the automated analysis of the recordings. The different classes of power system events must be defined and their distinctive characteristics must be extracted. This way, event-statistics (faults, switching operations, etc) can be obtained next to the already used disturbance-statistics (voltage dip, transient, etc) and information about the system's state can be extracted.

1.2 Outline of this thesis

This thesis consists of a summarising part followed by a number of papers either published or submitted for publication. The summarising part gives a short introduction on power system events and the objectives of this work. A summary of the papers is

given below.

The final goal of this project is the automatic classification of power system events. Towards this direction, this thesis focuses on a number of events that occur during power system operation and presents the results of the analysis of actual recordings. New classes of events are defined and the distinctive characteristics of each class are given. The guidelines for the development of a knowledge-based classification system, which utilises these features, are given in the summarising part.

Papers A and B present a new fault location technique for two and three terminal lines. The technique utilises the high frequency fault-clearing transients of voltage, which are measured on the line side of the circuit breaker. Two different approaches (in the time domain and frequency domain) are used in order to estimate the location of permanent faults. The method is tested with simulations using the Electromagnetic Transients Program (EMTP).

Paper C presents a method for the identification and classification of transients due to synchronised capacitor switching. Two types of synchronised switching for capacitors are considered: the zero-crossing method and the "5 msec" method. The basic concept of synchronised switching is the closing of each phase at certain instants and the wavelet transform is utilised to accurately locate these instants on the voltage waveforms. The algorithm, which is suggested for classification, considers also the case where the switching transients propagate through delta-star transformers. Measurements and simulations in EMTP are used to test the algorithm.

Paper D presents a new type of power system event that was observed during a monitoring program. It was found that transformer saturation might occur due to voltage recovery after a voltage dip. This type of event has not been presented before in the literature.

Paper E deals with two issues: first it presents different types of voltage dips as they were found in different power quality monitoring databases. The distinctive characteristics of each type that can be used for automatic classification are also identified. Second, using these characteristics a large number of recordings from a medium voltage network are classified and the results are presented. The most interesting results are: 1. Voltage dips due to transformer energising are a significant part of the power system events that were captured by the power quality monitors and 2. A large number of voltage dips due to faults are multistage, i.e. they present different levels of magnitude before the voltage returns to normal.

Chapter 2 Classification of power system events

The term power quality refers to a wide variety of electromagnetic phenomena that characterise the voltage and current at a given time and at a given location on the power system [1]. The increasing importance of power quality has made necessary the characterisation of the different phenomena that occur in voltage and current. This chapter gives the background of characterising these phenomena and the outline of the work that led to Papers C, D and E.

2.1 Power system events

A power system event is a recorded (or observed) current or voltage excursion outside the predetermined monitoring equipment thresholds [2]. Table 2.1 gives the different categories of the electromagnetic phenomena that a power system event might cause [1]. A power disturbance is a recorded (or observed) current or voltage excursion (event) which results in an undesirable reaction condition in the electrical environment or electronic equipment or systems. The term power problem refers to a set of disturbances or conditions that produce undesirable results for equipment, systems or a facility.

Categories	Typical spectral content	Typical duration	Typical voltage magnitude
1.0 Transients			
1.1 Impulsive			
1.1.1 Nanosecond	5 nsec rise	<50 nsec	
1.1.2 Microsecond	1 μsec rise	50 nsec-1 msec	
1.1.3 Millisecond	0.1 msec rise	>1 msec	
1.2 Oscillatory			
1.2.1 Low frequency	<5 kHz	0.3-50 msec	0-4 pu
1.2.2 Medium frequency	5-500 kHz	20 μsec	0-8 pu
1.2.3 High frequency	0.5-5 MHz	5 μsec	0-4 pu
2.0 Short duration variations			
2.1 Instantaneous			
2.1.2 Sag (dip)		0.5-30 cycles	0.1-0.9 pu
2.1.3 Swell		0.5-30 cycles	1.1-1.8 pu
2.2 Momentary			
2.2.1 Interruption		0.5 cycles-3 sec	<0.1 pu
2.2.2 Sag (dip)		30 cycles-3 sec	0.1-0.9 pu
2.2.3 Swell		30 cycles-3 sec	1.1-1.4 pu
2.3 Temporary			
2.3.1 Interruption		3 sec-1 min	<0.1 pu
2.3.2 Sag (dip)		3 sec-1 min	0.1-0.9 pu
2.3.3 Swell		3 sec-1 min	1.1-1.2 pu
3.0 Long duration variations			
3.1 Interruption sustained		>1 min	0.0 pu
3.2 Under-voltages		>1 min	0.8-0.9 pu
3.3 Overvoltages		>1 min	1.1-1.2 pu
4.0 Voltage unbalance		Steady state	0.5-2%
5.0 Wave distortion			
5.1 dc offset		Steady state	0-0.1%
5.2 Harmonics	0-100th harmonic	Steady state	0-20%
5.3 Inter-harmonics	0-6 kHz	Steady state	0-2%
5.4 Notching		Steady state	
5.5 Noise	Broadband	Steady state	0-1%
6.0 Voltage fluctuations	<25 Hz	Intermittent	0.1-7%
7.0 Power frequency variations		<10 sec	

Table 2.1. Categorisation of electromagnetic phenomena [1]

Table 2.2 gives the main characteristics of some important power system events and some of the phenomena related to them. In this thesis the first four events of Table 2.2 are considered. Measurements of these types of events are available and presented in Papers C and E.

<table>
<tr><th colspan="2" rowspan="2">Major Events</th><th colspan="3">Related phenomena</th></tr>
<tr><th>Protection operation</th><th colspan="2">Other</th></tr>
<tr><td rowspan="4">1</td><td rowspan="4">Faults</td><td rowspan="4">Fuse or circuit breaker operation</td><td colspan="2">10 different types of faults</td></tr>
<tr><td colspan="2">Voltage dip (single or multistage)</td></tr>
<tr><td colspan="2">Self-extinguishing faults</td></tr>
<tr><td colspan="2">Reclosing operation</td></tr>
<tr><td>2</td><td>Induction motor starting</td><td>No</td><td colspan="2">Voltage dip</td></tr>
<tr><td rowspan="2">3</td><td rowspan="2">Transformer energizing</td><td rowspan="2">No</td><td colspan="2">Voltage dip</td></tr>
<tr><td colspan="2">Saturation / Temporary increase in harmonic distortion</td></tr>
<tr><td rowspan="4">4</td><td rowspan="4">Capacitor energizing</td><td rowspan="4">No</td><td colspan="2">Increase in the (displacement) power factor and in rms voltage</td></tr>
<tr><td rowspan="2">Synchronised switching</td><td>Zero point switching (grounded systems)</td></tr>
<tr><td>“5 msec” delay (ungrounded systems)</td></tr>
<tr><td colspan="2">Permanent increase in harmonic distortion</td></tr>
<tr><td>5</td><td>Line energizing</td><td>No</td><td colspan="2">Synchronised switching</td></tr>
<tr><td>6</td><td>Reactor energizing</td><td>No</td><td colspan="2">Synchronised switching</td></tr>
</table>

Table 2.2. Some power system events and their characteristics

Regarding Table 2.2 two points must be highlighted:
1. Two types of events should be defined in terms of protection operation under normal conditions.

- Events for which the protection system operates. These events are faults. Table 2.3 contains the typical operating times for different types of fault clearing devices [3]. Reclosers and circuit breakers have a long delay due to the protection scheme that is employed (distance protection, differential protection etc.) and sends a trip command to the device as soon as a fault is detected. As explained in Paper E, the information that is given in Table 2.3 is important in analysing and grouping power system events that are related to faults.
- Events for which the protection does not operate (transformer energising, capacitor energising etc).

Type of fault clearing device	Minimum of clearing time in cycles	Typical time delay in cycles	Possible number of retries
Expulsion Fuse	0.5	0.5-120	None
Current limiting fuse	<0.25	0.25-6	None
Electronic recloser	3	1-30	0-4
Oil circuit breaker	5	1-60	0-4
SF6 or vacuum circuit breaker	2-3	1-60	0-4

Table 2.3. Fault clearing device operating times [3]

However, there are cases that protection fails to correctly identify a situation and operates although it should not. A typical example is transformer energising where the protection fails to recognise that the excessive currents are due to the energising and operates like in the case of a fault.

2. A power system event presents different features, depending mainly on the position of the monitor equipment with reference to the place where the actual event takes place. Fig. 2.1 shows two possible monitoring points for induction motor starting. Both monitoring points experience a voltage dip due to the induction motor starting. However, in the steady state, the current flowing through monitoring point M2 increases due to induction motor starting, but current flowing through monitoring point M1 does not.

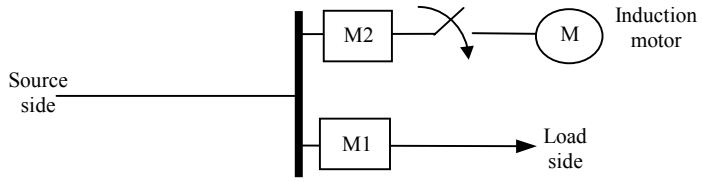

Fig.2.1. Different monitoring points for recording a power system event

2.2 Power quality monitoring -recordings

Power quality monitoring is necessary to characterise electromagnetic phenomena at a particular location of the network. The objective of monitoring can be [1]:

- the diagnosis of incompatibilities of the power system with the load.
- the evaluation of the electric environment at a part of the system in order to refine modelling techniques or to develop a power quality baseline.
- the prediction of future performance of load equipment or power quality mitigating devices.

The objectives of the monitoring for a certain project define the monitoring equipment to be used and the triggering thresholds of the monitors. Several monitors are commercially available offering different characteristics, i.e. in the settings, in the saving options or the communication capabilities.

Typical attributes obtained by most of the monitors:

- rms values of voltage and current
- total harmonic distortion
- harmonics of voltage and current

Typically, these attributes are calculated over a short period of time and then their averages are recorded by the monitor. However, there are monitors that according to their settings are able to record the actual waveforms of voltage and current. These types of recordings are the ones that are the subject of this thesis.

Several links have been established with utilities and research institutes in order to obtain recordings of power quality monitors. Through these links, a number of data is available. However, the recordings that are available rarely have a description or explanation. Therefore, they cannot always be explained. Further limitation in the analysis is the fact that information about the system, where the recordings are taken, is usually not available.

The analysis that is presented in this thesis is concentrated on voltage measurements. Actually, current measurements are not always available and the conclusions that are drawn in this thesis are mainly referred to voltage. Data that are presented and analysed in this thesis come from:

- Göteborg Energi Nät AB: monitors placed at 132 kV, 10 kV and 400 V systems.
- SINTEF Energy Research: monitors placed at 400V systems.
- Power quality monitors owned by the department of Electrical Power Engineering in Chalmers: placed at 400 V systems.
- IEEE web site [4]: data from medium voltage systems.
- Scottish Power: monitors placed at 33 kV and 11 kV.

2.3 Knowledge-based system for power system event classification

Several approaches have been used in the past for power system event classification [5] or disturbance waveform classification [6,7] using neural networks and artificial intelligence. However, this thesis presents the guidelines of a knowledge-based approach for a classification system for power system events.

Fig. 2.2 shows the voltage recording during a fault that is cleared in less than one cycle. Three parts can be recognised in this signal: the major event which caused the triggering of the monitor and must be the output of the classification and the parts of the signal before and after the major event (referred to as pre-event and post-event). Two more parts can be seen in the signal: the beginning and the end of the disturbance, referred to as minor events. The first minor event is the fault initiation and the second is the fault clearing operation. In general, the detection of minor events can be useful for the classification of major events. Minor events that are related to protection operation have time properties defined by the protection operation timing. In the example that is given in Fig. 2.2, the second minor event is fuse operation because no other type of protection could operate in less than one cycle according to Table 2.3.

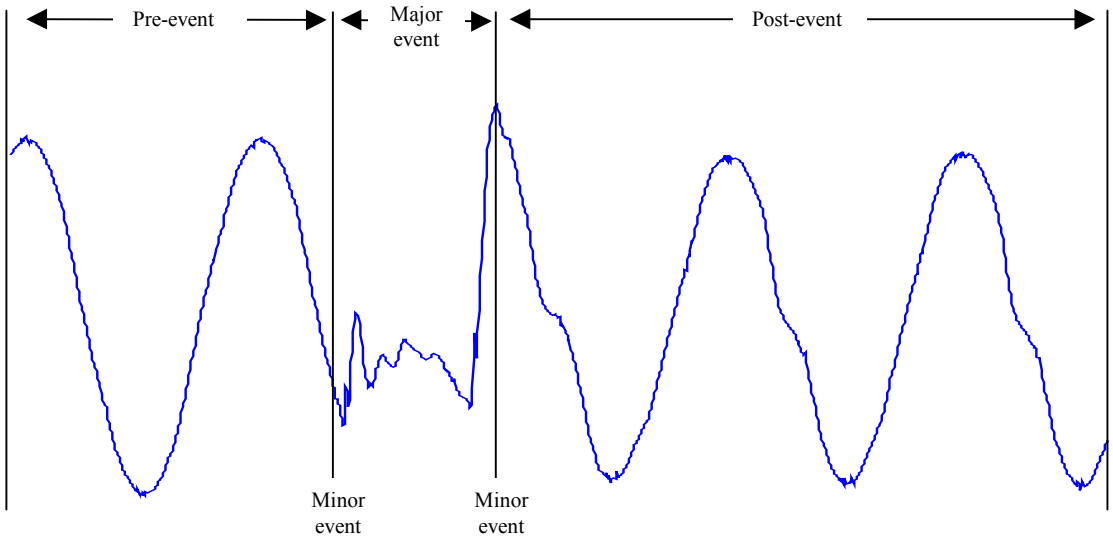

Fig. 2.2. Terminology for power system events

Paper C considers transients that are caused by capacitor energising when synchronised switching techniques are applied. It suggests an algorithm that can be used to detect and identify the event of capacitor energising, by detecting the minor events and their time sequence. The minor event in this case is the switching of each phase.

The pre-event and post-event parts of the signal can be used to classify recordings and identify related problems as in the case that is presented in Paper C, where the energising of a capacitor bank amplifies the harmonic distortion. Therefore, one more feature (increased harmonic distortion) is available for the identification of this power event. Other attributes that could be used are the power flows, the rms values of voltage and current and their phase angle (power factor).

Fig. 2.3 shows the structure of a knowledge-based system for power event classification. Four modules are recognised:

- Voltage dip classification: this is described in Paper E. It covers events whose main characteristic is a temporary decrease in the fundamental voltage magnitude. These are:
    - Faults - followed or not by protection operation
    - Induction motor starting
    - Transformer energising
- Synchronised switching classification: this is described in Paper C and covers the identification of synchronised switching techniques for capacitor energising. Two techniques are considered:
    - Zero crossing switching
    - “5 msec”-switching

  The same idea of detecting the switching instants in a closing sequence could be used for other events that utilise synchronised switching (line switching, reactor switching, transformer energising).
- Pre-event and post-event data comparison: as described above.

- Information about the system: the results of the three above mentioned modules can be combined with information about the system's operation characteristics. Such information are:
    - the protection system used and its time settings
    - the voltage control methods used (capacitors, reactors etc) and their characteristics (synchronised switching)

All the above information (the outputs from the voltage dip and synchronised switching classification modules as well as the system information and the comparison of the pre-event post-event data) can be incorporated in a set of rules that will classify the underlying event that caused the recording.

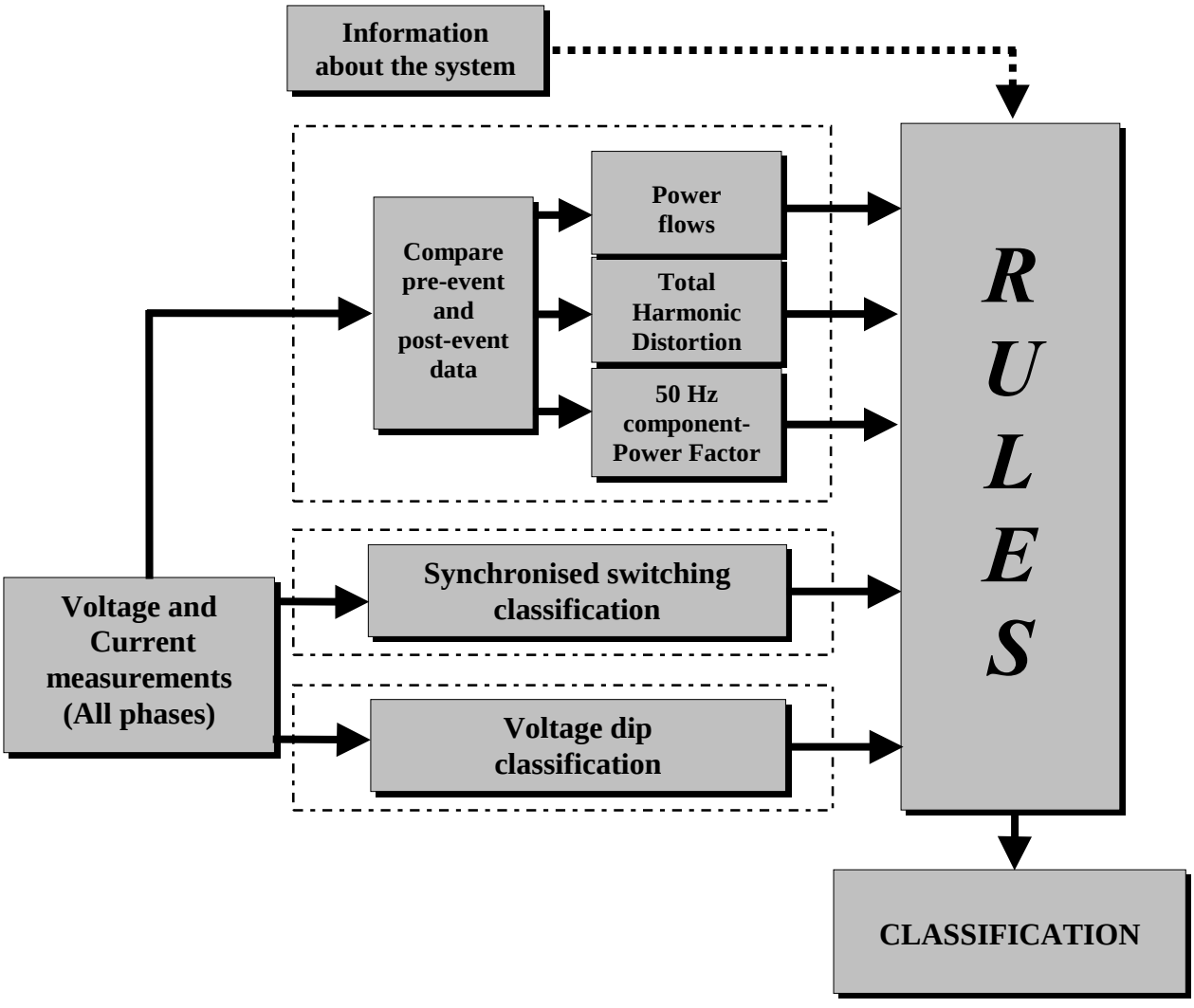

Fig. 2.3: Structure of the knowledge based system for power system event classification

2.4 Future work

The large size of the databases that are created by the power quality monitors drives the development of new tools for fast and efficient processing of the recordings. A rule-based system for automatic classification can be built that will utilise the results of the analysis and the features that were presented in section 2.3 and Papers C and E. The potential in using signal modelling and pattern recognition techniques must be examined. The classification can be extended to include power system events other than the ones that were presented in this thesis. Line switching, reactor switching, lightning are some examples of power system events that have not been treated yet.

All the measurements that are presented in this thesis were performed mainly in medium voltage networks, and only a few in low voltage networks. Although a number of the events that have been described so far took place in higher voltage levels and propagated to the rest of the system, measurements performed in high voltage systems are not available. Measurements from these networks (transmission and sub-transmission) will:

- increase the understanding of the events that are captured in medium voltage networks originating from higher voltage levels and the way that they propagate throughout the system.
- extend the list of the power system events that the classification system can consider.

The analysis of a large database (Paper E) showed that a large portion of the recordings is due to fault-induced voltage dips. However, a significant number of them cannot be described with a single magnitude and duration, because they contain multiple components. There is a recognised need to describe these types of voltage dips and include them in the power quality standards [8]. Further analysis is needed to extract more information on the characteristics of fault-induced voltage dips. The influence of the load, the protection operation and fault behaviour are some of the factors that can be included in the description of this type of voltage dips.

A power system event does not necessarily lead to a problem. However, when it does the source of the problem must be identified in order for corrective action to be taken. An example is capacitor switching: it could cause high overvoltages damaging for the customer's equipment [9] or increased harmonic distortion as described in Paper C. If more capacitors are connected in the system they might amplify the oscillation that is caused by the switching (the phenomenon is called voltage amplification [10]). Moreover, capacitors can even cause overvoltages during transformer energising [11]. Analysis can reveal the characteristics of such cases and diagnostic tools can be developed to identify these problems.

Power system protection and power quality mitigation equipment require classification of an event before it is completed. In addition, estimation of the steady state voltage must be done as fast as possible. Signal processing techniques can be investigated in order to achieve accurate and fast classification and estimation. Multiple models from the different types of events can be used. The performance of the different methods and models must be compared in terms of time.

2.5 References

[1] IEEE recommended practice for monitoring electric power quality, IEEE Std 1159-1995, Nov. 1995.

[2] The Dranetz Field Handbook for Power Quality Analysis. Dranetz Technologies Incorporated, Edison, New Jersey, 1991.

[3] Conrad, K. Little, C. Grigg: Predicting and preventing problems associated with remote fault-clearing voltage dips, IEEE Transactions on Industry Applications, vol. 27, no.1, January-February 1991, pp. 167 –172.

[4] IEEE web site: (http://grouper.ieee.org/groups/1159.2/testwave.html.)

[5] http://www.electrotek.com/PROJECTS/event.html: Power quality Diagnostic system – Event Classification Module.

[6] A.K. Ghosh, L.L. David: The classification of power system disturbance waveforms using a neural network approach, IEEE-Transactions on Power Delivery, vol. 10, no. 1, January 1995, pp. 109-115.

[7] S. Santoso, E. J. Powers, W.M. Grady, A.C. Parsons: Power quality disturbance waveform recognition using wavelet based neural classifier, IEEE PE-599-PWRD-01-1997.

[8] D.L. Brooks, R.C. Dugan, M. Waclawiak, A. Sundaram: Indices for assessing utility distribution system RMS variation performance, IEEE Transactions on Power Delivery, vol. 13, no. 1, January 1998, pp. 254 –259.

[9] V.E. Wagner, J.P. Staniak, T.L. Orloff: Utility capacitor switching and adjustable-speed drives, IEEE Transactions on Industry Applications, vol. 27, no. 4, pp. 645 –651.

[10] M.F. McGranaghan, G. Hensley, T. Singh, M. Samotyj: Impact of utility switched capacitors on customers systems – Magnification at low voltage capacitors, IEEE-Transactions on Power Delivery, vol. 7, no. 1, January 1992, pp. 645-651.

[11] J.F. Witte, F.P. DeCesaro, S.R. Mendis: Damaging long-term overvoltages on industrial capacitor banks due to transformer energization inrush currents, IEEE Transactions on Industry Applications, vol. 30, no. 4, July-August 1994, pp. 1107 -1115.

Paper A and B Fault location technique for two and three terminal lines using high frequency fault clearing transients

Abstract

This paper suggests that a voltage recorder, placed next to a circuit breaker, not as usual on the side of the substation, but on the side of the transmission line, may reveal the location of permanent faults. Two different approaches to estimating the fault location are presented here: a frequency domain approach and a time domain approach. These methods are tested and compared with simulations of typical transmission systems using the Electromagnetic Transients Program (EMTP). Two typical line configurations are considered: two terminal lines and three terminal lines.

Keywords

Transmission lines, fault location, spectrum analysis, discrete wavelet transforms.

AB.1 Introduction

Transmission lines suffer from short-circuit faults that can damage the lines as well as the equipment connected to them. Protection schemes are expected to operate and clear the fault by opening the circuit breakers that connect the line with the healthy part of the network. Reclosing schemes are used to bring the line back in operation if the fault is cleared. If all the reclosing attempts fail, the fault is assumed permanent and the circuit breaker stays open. In this case, a repair crew should be sent to the fault point. For efficient dispatch of repair crews high accuracy is needed in determining fault location. Unlike protective relays, which only need to detect whether a fault is in its zone of protection, fault location must give an accurate distance to the fault. This saves time and expense of the crews, often searching in bad weather conditions or at places that are difficult to reach.

Different fault location algorithms have been proposed that use voltage and current data or techniques based on the detection of travelling waves [1]. All proposed algorithms use voltages and currents between fault initiation and fault clearing. The algorithm proposed in this paper, uses the voltages at the line-side of the circuit breaker, after the breaker has opened. The transient due to opening of the breaker can reveal the location of permanent faults. Two different line configurations are considered to test the proposed algorithm: two-terminal and three-terminal A frequency domain approach and a time domain approach have been used for fault location using the fault clearing transient. This paper is an extension to a previous paper [2], where only two-terminal lines were considered.

AB.2 The frequency domain approach

AB.2.1 The concept

First we consider the two-terminal line system of Fig. 1. This is a typical system configuration and it has been used in the literature as a model for fault location estimation.

In the case of a fault at distance L, within the zone of protection of the protective relay, circuit breaker 1 (CB1) receives a trip signal from the relay and opens to clear the fault. This operation time varies between one cycle and more than one second. Due to the fault clearing operation of the circuit breaker, a surge is initiated and travels between an open circuit (circuit breaker open-reflection coefficient equals to 1) and a short circuit (fault-reflection coefficient equals -1), if the fault is still present.

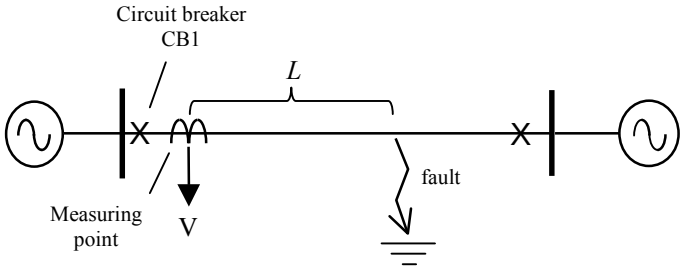

Fig. 1. Two terminal line system

When the surge hits the fault point, it is reflected with reversed sign and travels back to the open end of the line. Then it is reflected again from the open end but with the same sign and returns back to the fault point. Since the duration of this complete cycle is 4τ, (τ is the propagation time of the surge from the open end to the fault point) the main component of the voltage signal after the CB1 opening has a frequency equal to [3]:

$$f = \frac{1}{4\tau} \qquad (1)$$

so that the distance to the fault may be obtained:

$$L = \frac{c}{4f} \qquad (2)$$

where c is the propagation speed of the surge. Simulations have been performed for a system like the one shown in Fig. 1. Fig. 2 shows the voltage on the line-side of CB1 during a fault, including the fault clearing operation (CB1 opens). More frequency components might be present due to other waves that propagate along the line, however, the frequency given by (1) is the dominant one.

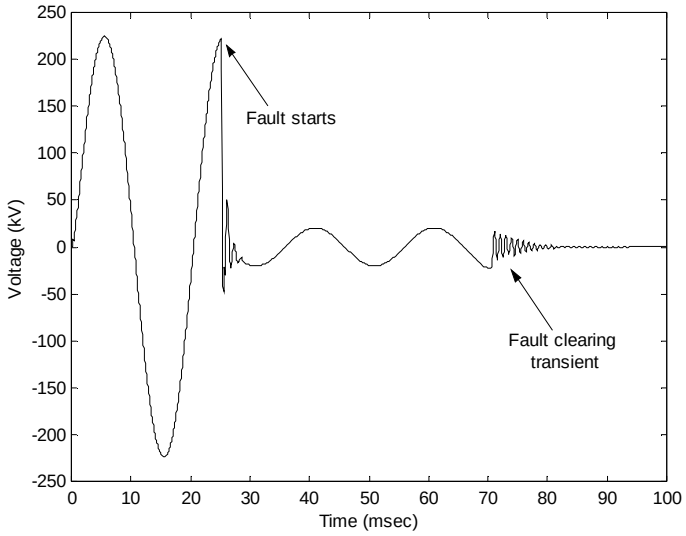

Fig. 2. Voltage during a fault clearing operation measured on the line-side of the circuit breaker for a two-terminal line

AB.2.2 Spectrum estimation

The estimation of the fault location related frequency in (2) is a task that should be considered separately because:

- Other frequencies (e.g. due to reflections of the initiated surge elsewhere in the system), may be present making the estimation of the dominant frequency more difficult. This is not the case for a three-phase fault but for all the other types of faults.
- This frequency must be estimated by using a small number of samples because the waves initiated by the circuit breaker operation are damped fast.
- During a circuit breaker operation, the three phases do not clear the current simultaneously. The current clears when it crosses through zero. When one phase is switched off, a transient is induced to the other phases posing an extra problem for the spectrum estimator.
- The accuracy of frequency estimation affects the accuracy of fault location so a method is needed that can provide high resolution.

Three spectrum estimation methods are considered and compared:
Welsh's method [4]: The power spectrum of a stationary signal can be estimated by using the discrete time Fourier transform and calculating the magnitude square of it. For a stationary signal the estimate is obtained by splitting the signal into segments, computing the spectrum for each segment and averaging these spectrums. In Welsh's method the segments are overlapped and the data in each segment is multiplied by a window function.

Autoregressive (AR) Spectrum Estimation [5]: This is a parametric method based on modelling the signal as the output of a linear system characterised by a rational system function:

$$H(z) = \frac{1}{A(z)} = \frac{1}{1 + \sum_{k=1}^{p} a_k z^{-k}} \qquad (3)$$

where p is the order of the model. After a_k are estimated, the power spectrum of the signal is computed from $|H(e^{j\omega})|^2$. Different ways of estimating a_k exist. For our tests, Burg's approach was used, because the estimated AR spectrum has a high resolution in low noise data and a good spectral fidelity for short data records. Fig. 3 shows the spectrum of voltage after fault clearing using this method. The maximum peak of this spectrum corresponds to the frequency that should be used in (2).

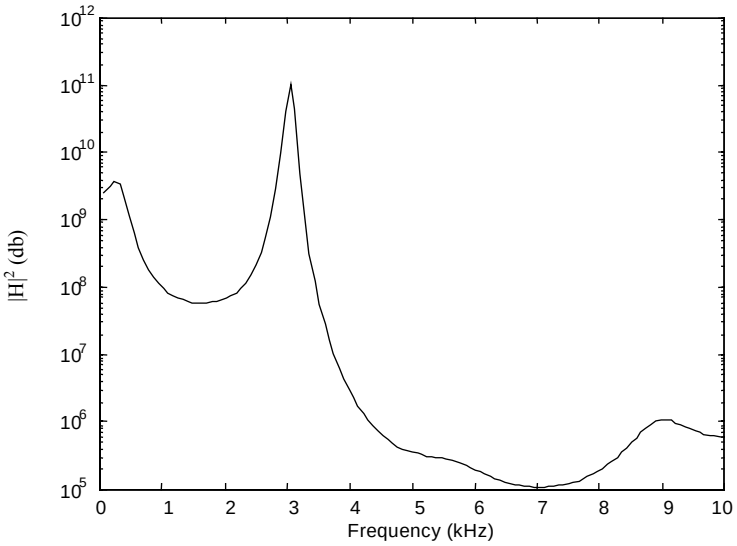

Fig. 3. Spectrum of voltage after fault clearing using AR spectrum estimation

Multiple Signal Classification (MUSIC) [6]: This is a method of spectrum estimation based on eigenvalue analysis of the signal autocorrelation matrix. It categorises the information based on the correlation of the data matrix, assigning information to either a signal subspace or a noise subspace. This method has also been used for high-resolution beamforming.

AB.2.3 Cases

The method has been tested for the above mentioned system configuration using the Electromagnetic Transients Program (EMTP). Several fault types and fault resistances have been considered. The frequency dependent model (JMARTI's model) was used for modelling the 400 kV transmission line. The length of the transmission line was 86 km and the propagation speed was calculated from the simulations. A sampling frequency of 20 kHz was used in the simulations. Simulations were also carried out using higher sampling frequencies. However, the results did not show any improvement. Interpolation techniques were also tried but the results did not justify such an approach. So, for the frequency domain approach we kept the sampling frequency to 20 kHz.

Table 1 gives the results for several cases using the three spectrum estimation methods mentioned above. The results are good and do not promote particularly any of these methods. The same length of data (200 samples) was used in spectrum estimation for all cases. The analysis window started at the data sample, which corresponded to the time instant of circuit breaker opening. For Welsh's method, a Hamming window was used with 50% overlap. For Burg's approach the order of the AR-model was set to p=20. For the MUSIC method the number of eigenvectors in the signal subspace was set to 8.

Case	Distance (km)	Distance measured using spectrum estimation (km)		
		Welsh's	AR	MUSIC
Single phase Fault	64.16	63.90	61.33	63.90
Double phase fault	64.16	58.34	66.17	67.00
Double phase to earth fault	64.16	61.00	61.55	63.90
Three phase to earth fault	64.16	63.00	61.49	63.90
Single phase fault Fault resistance is 10 ohms	64.16	63.90	61.33	63.90
Single phase fault Fault resistance is 100 ohms	64.16	70.00	74.33	71.38

Table 1. Fault location estimation using spectrum estimation

AB.3 The time domain approach

AB.3.1 Discrete wavelet transform

Discrete Wavelet Transform (DWT) is a time-frequency signal analysis tool. It finds applications in different areas of engineering due to its ability to analyze the local discontinuities of signals [7, 8]. One way to interpret DWT is based on a filter bank shown in Fig. 4. A filter bank consists of multilevel of high-pass (H) and low-pass (L) filters that split the signal into the so-called details and approximations or different frequency bands. There are many different types of wavelet filters. In this paper Daubechie's wavelet of length 2 was used because of its good time localization properties [7].

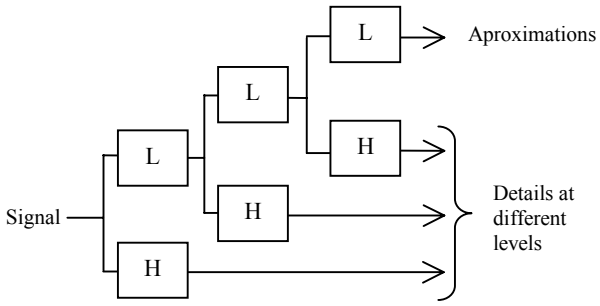

Fig. 4. Filter bank interpretation of DWT

AB.3.2 Discrete wavelet transform for travelling wave arrival detection

Consider the case of the double feed system and a single-phase fault at 64.16 km. The detailed signal from the lowest level of the DWT after circuit breaker opening is shown in Fig. 5. For this case a sampling frequency of 40 kHz is used.

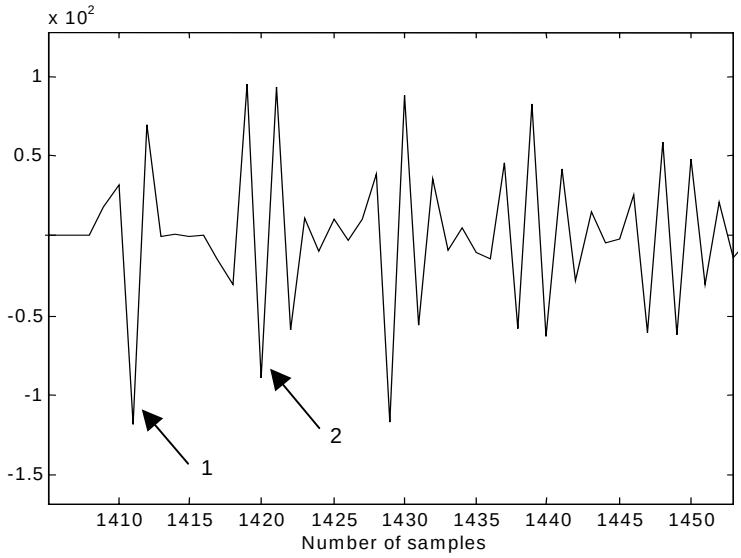

Fig. 5. DWT of voltage-lowest level details (Sampling frequency is 40 kHz)

Spike 1 corresponds to the instant that the circuit breaker opens and spike 2 corresponds to the instant that the reflected surge returns from the fault point of the line. The time elapsed between spike 1 and spike 2 (τ_{12}) is twice the propagation time of the surge from the open end to the fault point. So the distance L to the fault is given by:

$$L = \frac{1}{2} c\tau_{12} \qquad (3)$$

For the above mentioned example this is 63.75 km. Compared with the results obtained by the frequency domain approach, the time domain approach does not present an

improvement. However, the motivation for this approach is explained in the next section, where we consider three terminal line systems.

For detailed signals at higher levels, these two spikes are not so obvious as in the lowest level due to the lower time resolution. Therefore, only detailed signals from the lowest level are used. The accuracy of this approach is mainly dependent on the sampling frequency of the voltage recorder. The higher the sampling rate, the smaller the distance that one sample corresponds to and therefore, the more accurate the fault location estimation. In order to increase the accuracy of the time domain approach, interpolation techniques were used. This way the sampling frequency can be increased, however, the results did not become better.

AB.4 The three terminal line case

AB.4.1 About the frequency domain approach

Fault location in a three terminal line system (Fig. 6) is similar to that in the two terminal line systems that we described already. The main difference is that, in the three terminal line case, the frequency approach cannot be used. The reason is that the T point might be between the open end of the line (after circuit breaker opening) and the fault. In the two terminal line case, a surge travels between two points, of reflection coefficients 1 and –1. In the three terminal line case this in no longer a valid assumption. Therefore, for three terminal line systems the time domain approach is applied.

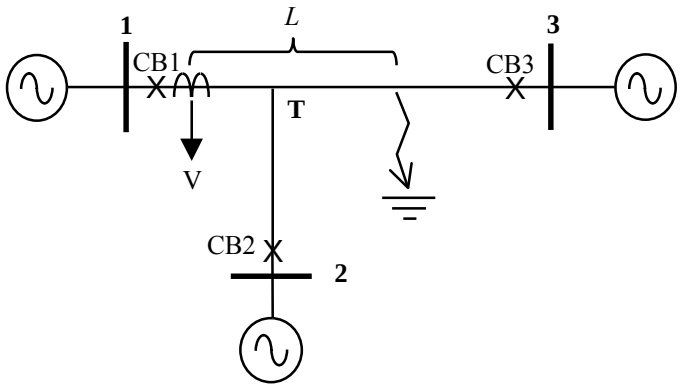

Fig. 6. The three terminal line case (T-1)=22 km (T-2)=38 km (T-fault)=64 km (T-3)=86 km

When the circuit breaker opens, the initiated surge will travel along the lines and it will be reflected at a number of fixed points as well as the fault. The distance to the fixed points is known, and therefore, the reflection at the fault can be distinguished from the other reflections. Two different cases are treated below:

- measurements from all three terminals are considered and the time domain approach is applied
- measurements from only one terminal are considered and the time domain approach is

applied.

AB.4.2 Measurements from all three terminals

Consider the system of Fig. 6 and a single phase to earth fault. In order to increase the time resolution a sampling frequency of 200 kHz was used in the simulation. If all circuit breakers (CB1, CB2 and CB3) open and measurements are taken as before (next to the circuit breaker that opens but on the line side of the substation) then two cases exist. The first case is that the circuit breaker that opens corresponds to the branch where the fault occurs. The second case is that the circuit breaker that opens does not correspond to the faulty branch.

In the first case, the time domain method as it is applied in the two terminal line system will directly give the distance to the fault. Fig. 7 shows the fault-clearing transient of voltage when circuit breaker 3 (CB3) opens and Fig. 8 shows the detailed signal from the lowest level of the DWT of this transient. Using the time that has elapsed between spikes 1 and 2, the distance that is calculated using (3) is 22.70 km which is close to the distance from CB3 to the fault (22 km).

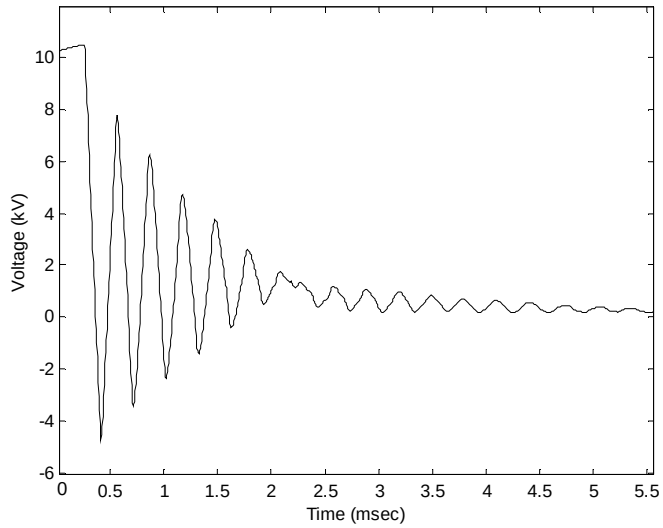

Fig. 7. Voltage of the faulted phase on the line side of CB3 when CB3 opens

In the second case the time domain approach will give the distance to the T point because this is the first point that the surge (initiated by the opening of the circuit breaker) meets. Fig. 9 shows the fault clearing transient of voltage when circuit breaker 2 (CB2) opens and Fig. 10 shows the detailed signal from the lowest level of the DWT of this transient. Using the time that has elapsed between spikes 1 and 2, the distance that is calculated using (3) is 38.25 km, which is the distance from CB2 to the T point (38 km).

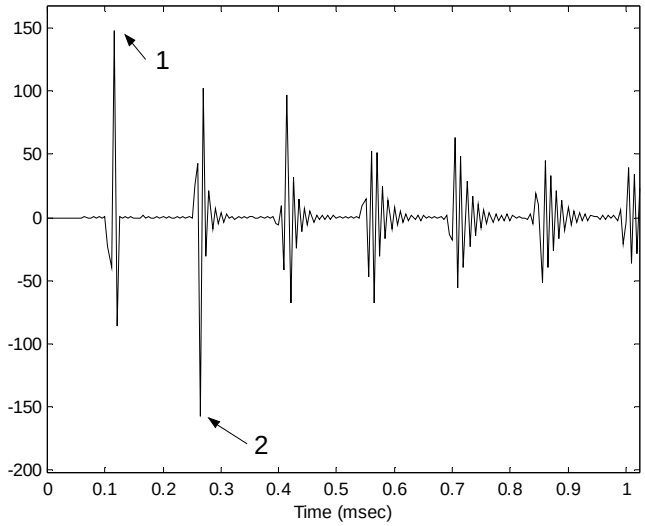

Fig. 8. Details from the lowest wavelet level of the fault clearing transient of voltage when CB3 opens

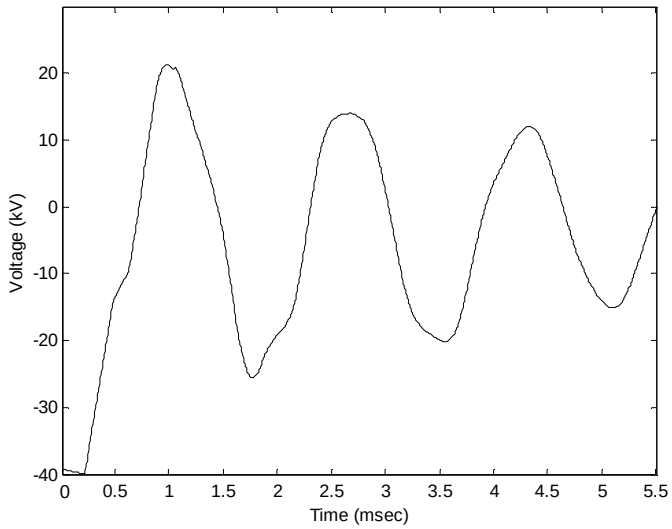

Fig. 9. Voltage of the faulted phase on the line side of CB2 when CB2 opens

Circuit breaker 1 (CB1) also belongs to the second case. If measurements are available from the opening of this circuit breaker, then the time domain approach will give the distance of CB1 to the T point.

Summarising, the time domain approach can be applied to three terminal line systems if measurements are available from all three terminals. Two distances will be obtained: the distance to the fault and the distance to the T point. The distance to the T point is known so fault location is possible.

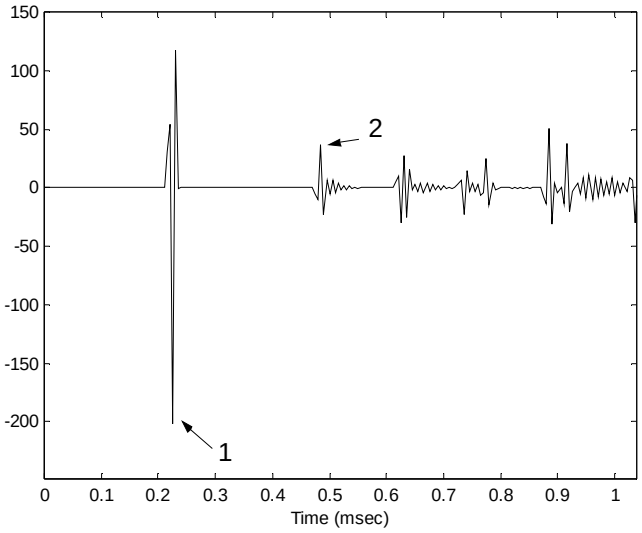

Fig. 10. Details from the lowest wavelet level of the fault clearing transient of voltage when CB2 opens

AB.4.3 Measurements from only one terminal

Here we consider the problem of fault location when measurements from only one terminal are available. In this case the analysis of the fault clearing transient should be extended up to the instant the initiated surge returns to the measuring point after being reflected at the fault point. In such an analysis all the fixed distances of the system (remote ends and T point) must be taken into account.

We again use the system of Fig. 6 and consider measurements obtained when circuit breaker CB1 opens. The fault-clearing transient as measured at the line-side of CB1 is given in Fig. 11. Fig. 12 shows detailed signal from the lowest level of the DWT of the fault clearing transient. Five spikes can be identified. The first spike corresponds to the opening of the circuit breaker. By calculating the time that has elapsed from the first point for each peak of Fig. 12 the distance that each travelling wave has covered can be calculated. Then, the calculated distances are compared with the distances of the fixed points of the system. The following case is possible: a travelling wave that is reflected twice at the same point and reaches the measuring point before the arrival of the travelling wave that is reflected to the fault.

For the case that we consider, the following distances were calculated:
Spike 2: 43.93 km
Spike 3: 87.87 km
Spike 4: 121.01 km
Spike 5: 166.65 km
Using these distances and comparing them with the distances to the fixed points, the following conclusions are made:
Spike 1 corresponds to the opening of the circuit breaker with busbar 1.
Spike 2: Travelling wave initiated by circuit breaker opening arrives after it is reflected at T point.
Spike 3: Travelling wave arrives after it is reflected at T point for the second time.

Spike 4: Travelling wave arrives after it is reflected at remote end 2.
Spike 5: Travelling wave arrives after it is reflected at the fault point, since there is no point to correspond to such a distance. So, estimated distance to the fault is 83.32 km (84 km is the correct one).

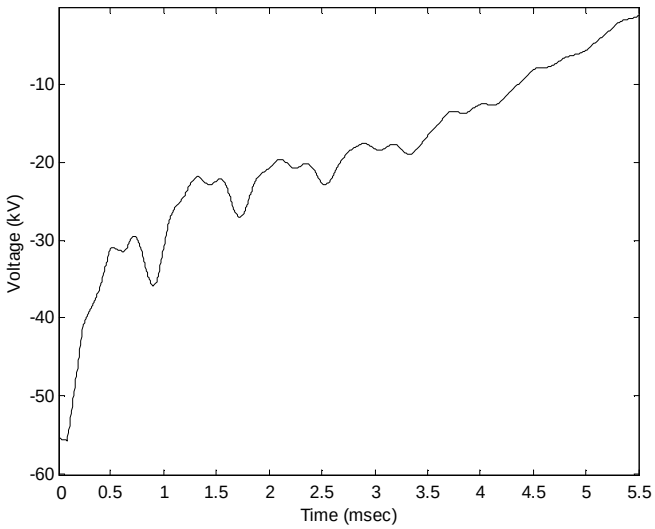

Fig. 11. Voltage of the faulted phase on the line side of CB1 during fault clearing

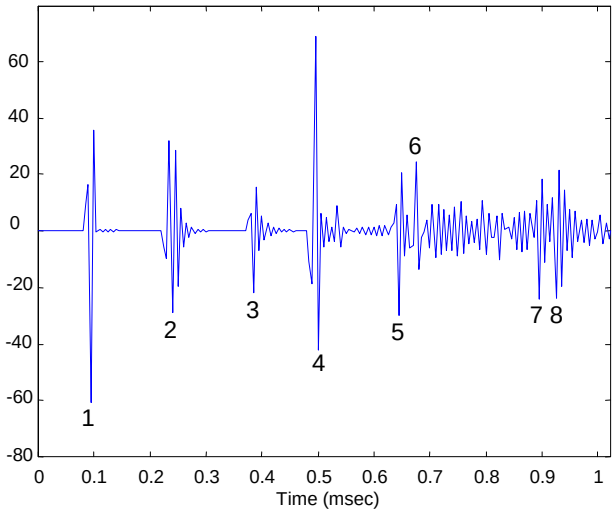

Fig. 12. Details from the lowest wavelet level of the fault clearing transient of voltage when CB1 opens

A simple algorithm may proceed as follows:
Step 1: detection of travelling wave arrival using DWT.
Step 2: calculation of the propagation time and the corresponding distance that each travelling wave has covered. If the fault is between the voltage recorder and the T point then the problem reduces to a problem similar to the two terminal line case. That means that the second spike will give a distance that is shorter than the T point.
Step 3: comparison of these distances with the fixed distances of the system. These points

are the T point and the remote ends of the system. The distance to the fault is the first distance that does not match to any of the distances to the fixed points.

AB.4.4 Further considerations

We should highlight here the importance of a high sampling frequency. High sampling frequency (as the one used in our simulation) does not only increase the accuracy of the approach as we mentioned already, but also makes the identification of the different spikes possible as in Fig. 12.

Finally, more aspects should be taken into account when measurements from only one terminal are available:
1) special attention should be given to cases where a fault occurs (as in Fig. 13), where the distance to the fault (L) is larger than the distance of the measuring point to a fourth busbar ($L>d_1+d_2$). That means that a travelling wave from busbar 4 arrives at busbar 1 before the travelling wave from the fault. In this case point 4 should be taken into account as one more fixed point.
2) The distance to the fault is not enough to locate a fault in a three terminal system. The branch of the system must be known as well. However, travelling waves will be mostly reflected at the fault point and will not propagate across it and towards the remote end. Therefore, there will be no reflections at the measuring point from the remote end of the branch of the fault. This is the case that we considered above. Spikes 6,7 and 8 do not correspond to a reflection from the remote end 3 for the system of Fig. 6.

AB.5 Conclusions

This paper proposes a new way of estimating the location of permanent faults in transmission lines. It requires a voltage recorder placed next to a circuit breaker on the side of the transmission line. The transient that results from the fault clearing operation of the circuit breaker is used to detect the position of the fault.

Two different methods have been described and tested using cases simulated in EMTP. The first method, the frequency domain approach is based on spectrum estimation. Three different spectrum estimation methods were used. The results are equally good for all three methods and not promote any of them. The second method is a time domain approach and utilises the discrete wavelet transform to detect the discontinuity from the detailed signals. Its accuracy is highly dependent on the sampling frequency used.

The time domain approach was applied to a three terminal line system when measurements from all three terminals are available and when measurements from only one terminal are available. By knowing the lengths of the branches of the system, fault location is possible. Finally, the limitations of the method are discussed. The approach shows strong potential in the solution of the fault location problem. However, real measurements are needed to verify the results that are presented in this paper.

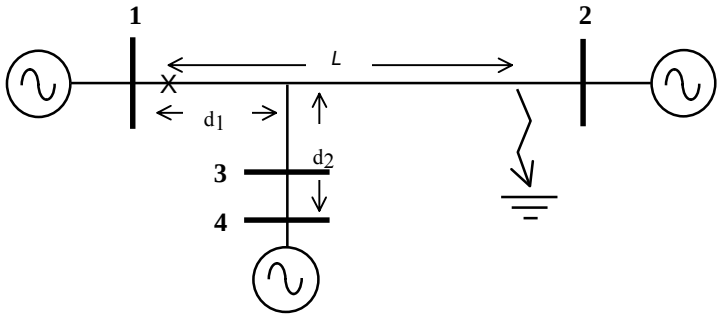

Fig. 13. A special case for the three terminal line

AB.6 References

[1] M.S. Sachdev (Editor): Advances in microprocessor based protection and communications, IEEE Tutorial course 97TP120-0.

[2] E. Styvaktakis, M.H.J. Bollen, I.Y.H. Gu: A fault location technique using high frequency fault clearing transients, IEEE Power Engineering Letters, May 1999, pp. 58-60.

[3] G.W. Swift: The spectra of fault induced transients, IEEE-Transactions on Power Apparatus and Systems, vol. 98, no. 3, May-June 1979, pp. 940-7.

[4] P.D. Welsh: The use of fast Fourier transform for the estimation of power spectra: A method based on time averaging over short, modified periodograms, IEEE Transactions on Audio Electroacoustics, vol. 15, June 1967, pp. 70-73.

[5] S.M. Kay, S.L. Marple: Spectrum analysis - a modern perspective, Proceedings of the IEEE, vol. 69, no. 11, November 1981, pp. 1380-1419.

[6] R.D. Schmidt: Multiple emitter location and signal parameter estimation, IEEE Transactions on Antennas and Propagation, vol. 34, March 1986, pp. 276-280.

[7] G. Strang, T. Nguyen: Wavelets and Filter Banks, Wellesley-Cambridge Press 1996.

[8] I.Y.H. Gu, M.H.J. Bollen: Time-Frequency and Time-Scale domain analysis of voltage disturbances, to appear in IEEE Transactions on Power Delivery 2000.

Paper C Classification of power system transients: Synchronised switching

Abstract

This paper presents a new method for the identification and classification of transients due to synchronised switching in three-phase systems. Signal processing techniques are introduced to detect the switching actions in the individual phases. The proposed method enables detection and classification of synchronised capacitor switching events. This in turn will lead to a reduction in the amount of data to be reported from a power quality survey.

Keywords

Power system monitoring, capacitor switching, switching transients, signal processing, wavelet transforms.

C.1 Introduction

Power quality monitoring easily leads to large amount of data [1,2]. The vast majority of data is often due to events of no direct interest to the monitoring project. Even if this data may be stored for future analysis, the reporting could be limited or even completely absent. Examples of such events are load switching, transformer energising, and capacitor energising. Especially when synchronised switching is used, the latter two are of minor importance. This paper focuses on transients that are produced by synchronised switching for capacitor energising. An algorithm is proposed for identification and classification of the different types of synchronised switching. The algorithm extracts the point on the wave where the switching action takes place for each phase (minor event), as well as the type of synchronised switching.

Synchronised switching causes small disturbances, and the proposed algorithm utilises the wavelet transform to locate the switching of individual phases on the voltage waveform. The suggested classification scheme utilises a set of rules based on the information extracted from the wavelet analysis and is robust and accurate. Classification is extended to include the case where the produced transients propagate in the system through delta-star transformers.

The algorithm is tested using measurements performed at 400 V and 10 kV by Göteborg Energi Nät AB (GENAB), the power utility of the city of Göteborg in Sweden. The monitors of GENAB capture a good number of events due to capacitor switching, which is a usual operation in this network. Simulations in the Electromagnetic Transients Program (EMTP) are used when real measurements are not available.

C.2 Background

Capacitor energising is used for power factor correction and voltage control. Drawbacks of the method are overvoltage transients and harmonic resonance. Synchronised switching is used to minimize the overvoltages that capacitor energising might cause [3].

C.2.1 Synchronised capacitor energising

Two different methods of synchronised switching for capacitor energising are reported in the literature. The first method employs switching of each phase separately when voltage crosses zero [4] as shown in Fig. 1a where the angles shown are with reference to the first phase which is switched. Fig. 1b shows the phase-to-ground voltage waveforms (obtained from an EMTP simulation) during capacitor energising. Steps 1,2 and 3 show the point where each phase is switched. This method will be referred to as zero-crossing capacitor energising.

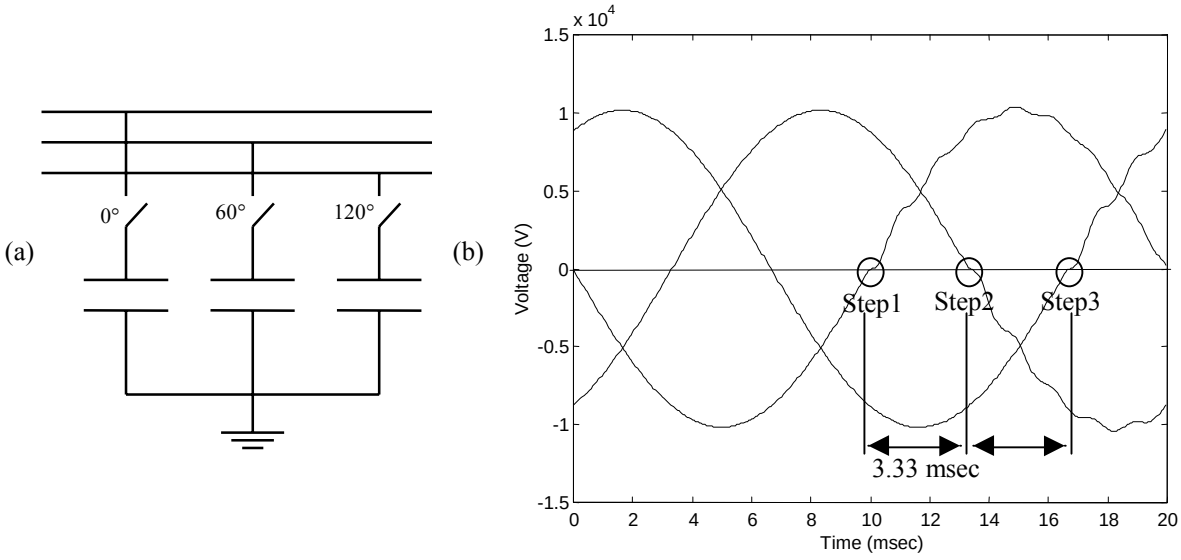

Fig. 1. (a) Sequence of switching and (b) phase-to-ground voltages during zero-crossing capacitor energising

The second method is applied to non-grounded star-connected capacitor banks in medium voltage networks [5]. Fig. 2 shows the sequence of switching (the angles shown correspond to the phase-phase voltage of the phases that are switched first) and the corresponding phase-to-ground voltage waveforms (obtained from an EMTP simulation). This method will be referred to as "5 msec"-capacitor energising. The closing sequence of this method is as follows: if the capacitor bank is uncharged, two phases close simultaneously when the voltage between them is zero (step 1 in Fig. 2b). Then the voltage of the star point of the capacitor bank becomes the average of the voltages of the two phases that were connected. This star point voltage has a zero voltage crossing after 90° (5 msec in a 50 Hz system), which is also the case for the third phase voltage. So to be able to minimise capacitor energising transients, it is necessary to have the third pole delayed with 5 msec (step 2 in Fig. 2b).

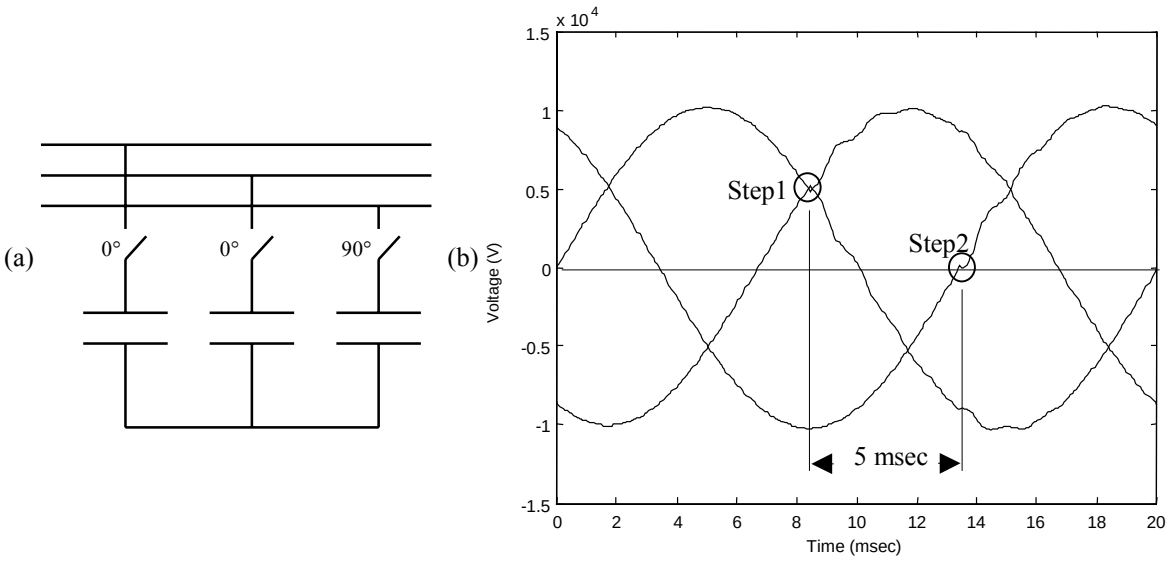

Fig. 2. (a) Sequence of switching and (b) phase-to-ground voltages during "5 msec"-capacitor energising

C.2.2 Discrete wavelet transform

The Discrete Wavelet Transform (DWT) is a time-frequency signal analysis tool [6]. It finds applications in different areas of engineering, due to its ability to analyze the local discontinuities of signals. Recently DWT has been used for the analysis of power engineering problems [7]. One way to interpret DWT is based on a filter bank as shown in Fig. 3. A filter bank consists of multilevel of high-pass (H) and low-pass (L) filters that split the signal into the so-called details and approximations or different frequency bands-levels as shown with dashed lines in Fig.3.

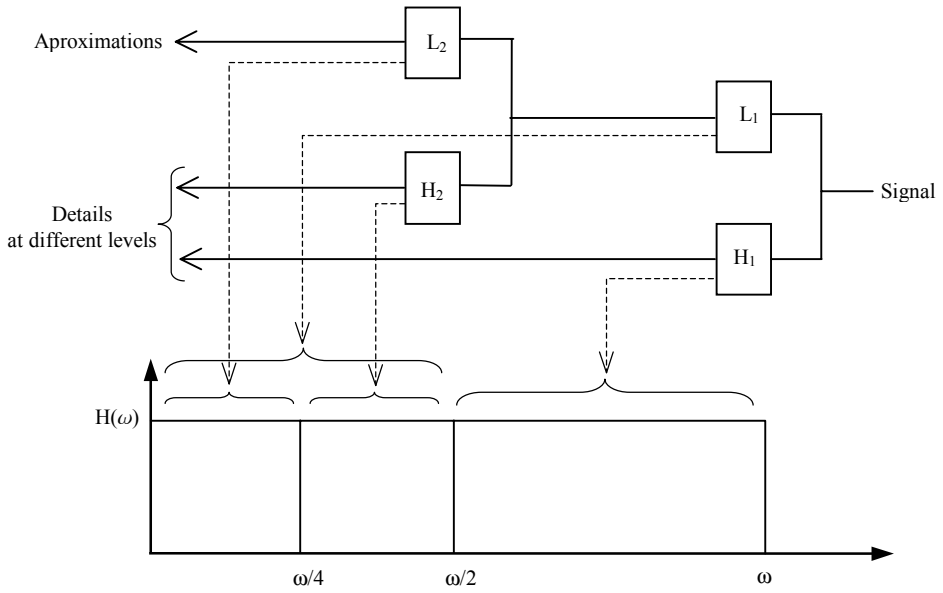

Fig. 3. Filter bank interpretation of DWT

In this paper, the DWT has been employed to detect the exact point where the switching of each phase takes place, and Daubechie's wavelet of length 4 was used [6]. The switching of each phase causes a transient of a certain frequency and the aim of using DWT is to reveal the exact instant in the corresponding frequency level. The Lowest Wavelet Level (LWL) was found to be adequate for detection purposes.

C.3 Analysis of synchronised switching events

C.3.1 Zero-crossing capacitor energising

Fig. 4 shows the phase-to-ground voltages during zero-crossing synchronised switching and the corresponding LWL of them. The waveforms were obtained from an EMTP simulation of a medium voltage (10 kV) system and the switching of a star connected grounded capacitor bank. The maximum of each LWL is found and a circle is plotted at the corresponding point of the phase-to-ground voltage waveform, for each phase. The switching event is clearly observable using the LWL, even though it is not very clear in the voltage waveform. The time difference between two sequential maxima is 3.33 msec (50 Hz system).

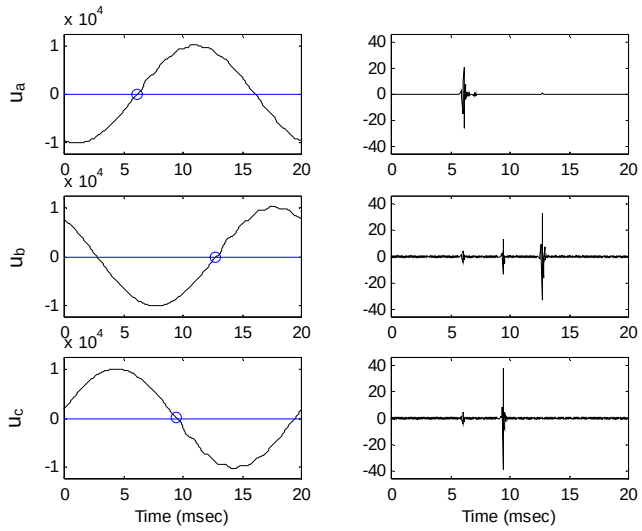

Fig. 4. (left) Phase-to-ground voltages during zero-crossing capacitor energising (EMTP simulation) (right) LWL

C.3.2 "5 msec"-capacitor energising

Fig. 5 shows the phase-to-ground voltages during "5 msec"-capacitor energising and the corresponding LWL of them. The waveforms were obtained from an EMTP simulation of a medium voltage (10 kV) system. The maximum of each LWL is found and a circle is plotted at the corresponding point of the phase-to-ground voltage waveform. The switching event for each phase is again clearly detected using the LWL. In phases b and c two spikes are present; one due to the switching of these two phases and one due to the switching of the third phase (phase-a) 5 msec after. However, for the phases b/c the first switching produces the strongest transient and this is the one that is detected using the maximum of the corresponding LWL.

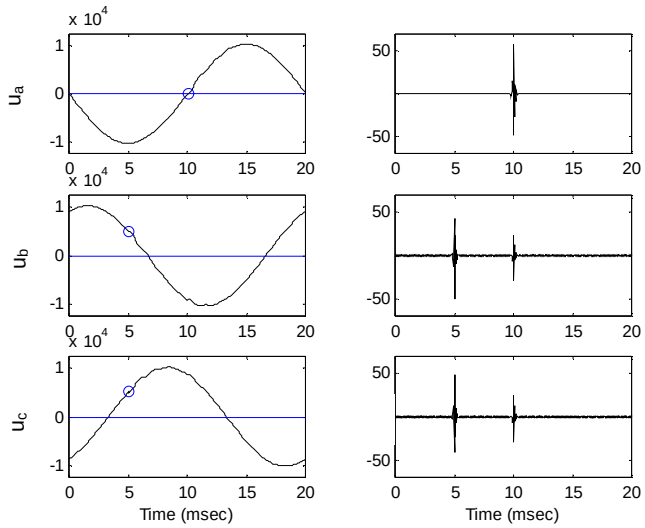

Fig. 5. (left) Phase-to-ground voltages during "5 msec"-capacitor energising (EMTP simulation) (right) LWL

However, a small change in the switching instants can change this and make the second transient the largest for all phases. Fig. 6 shows the phase-to-ground voltage measurements for such an event in a 10 kV network. In this measurement, the phase-c is switched delayed but shortly after voltage zero. This results in a transient for the other two phases larger than the one caused by the first switching action. Therefore, the maximum of the LWL of phase-to-ground voltages is not enough for classification purposes. The following features were observed both in the simulations and measurements:

1. The simultaneous switching of the two phases (step 1) does not cause a transient in the third phase.
2. The transients that are produced in these phases are anti-symmetric (same waveshape-opposite direction).
3. The switching of the third phase (step 2) causes the same transient in the other two phases (same waveshape-same direction).

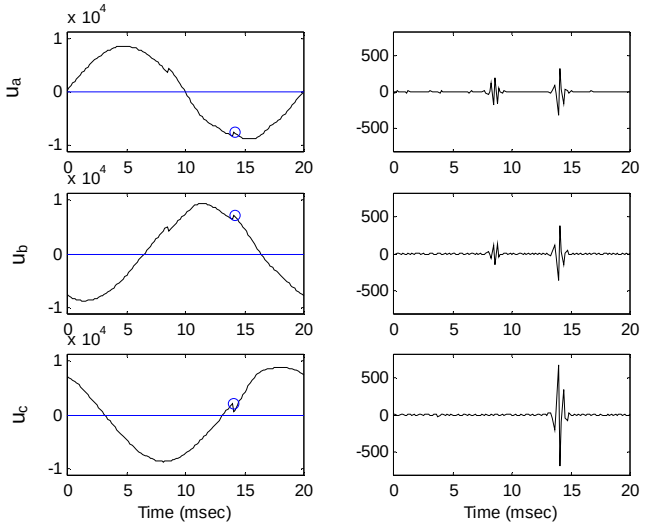

Fig. 6. (left) Phase-to-ground voltages during "5 msec"-capacitor energising (data provided by GENAB) (right) LWL

These features show that using the phase-to-phase voltages, waveforms can be created that contain only one major transient. By finding the position of this transient, classification becomes possible. Fig. 7 shows the phase-to-phase voltages and the corresponding LWL. The phase-to-phase voltage u_{ab} has its maximum of LWL at zero (step 1) and no transient due to the switching of phase-c (the transient that is caused in phase-a and phase-b by the switching of phase-c is eliminated in the phase-to-phase voltage u_{ab}).

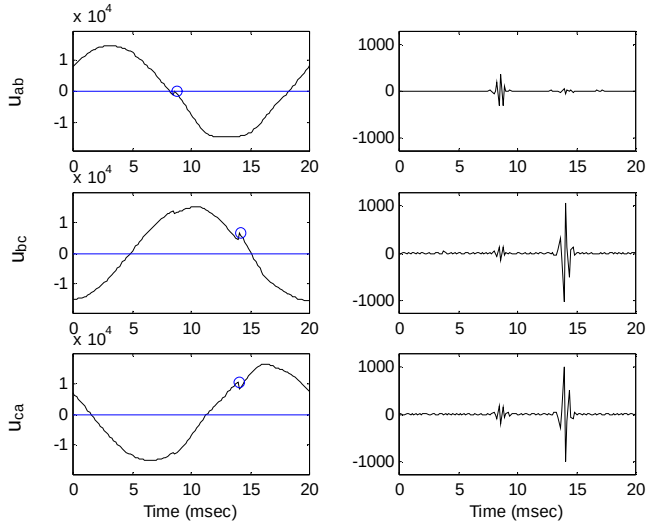

Fig. 7. (left) Phase-to-phase voltages during "5 msec" capacitor energising (data provided by GENAB) (right) LWL

Summarising, for the "5 msec"-capacitor energising case, both phase-to-ground voltages and phase-to-phase voltages must be used. The maximum of one of the LWL of one of the phase-to-phase voltages (u_{ab} in Fig. 7) must be close to zero and the maximum of the LWL of the remaining phase-to-ground voltage (u_c in Fig. 6) 5 msec (90°) after.

C.4 Propagation of synchronised switching transients

The transients that are due to synchronised switching are of low energy and are damped when they propagate in the system. However, since the switching actions take place in a substation they might be measured after they pass through a transformer. The case that is investigated here is the propagation of these transients through a delta-star transformer (Fig. 8), a typical transformer configuration for medium to low voltage. The delta-star transformer produces at the lower voltage side the differences of the voltages at the higher voltage side. If u_{1H}, u_{2H}, u_{3H} are the phase-to-ground voltages of the three phases at the higher voltage side of the delta-star transformer, then at the lower voltage side the following voltages will be measured (ignoring the transformer ratio):

$$\begin{aligned} u_{1L} &= u_{1H} - u_{2H} \\ u_{2L} &= u_{2H} - u_{3H} \\ u_{3L} &= u_{3H} - u_{1H} \end{aligned} \qquad (1)$$

As before, the phase-to-phase voltages are also used for classification. These are obtained

by subtracting the measured voltages:

$$u_{1pp} = u_{1L} - u_{2L} = u_{1H} + u_{3H} - 2\,u_{2H}$$
$$u_{2pp} = u_{2L} - u_{3L} = u_{2H} + u_{1H} - 2\,u_{3H} \qquad (2)$$
$$u_{3pp} = u_{3L} - u_{1L} = u_{3H} + u_{2H} - 2\,u_{1H}$$

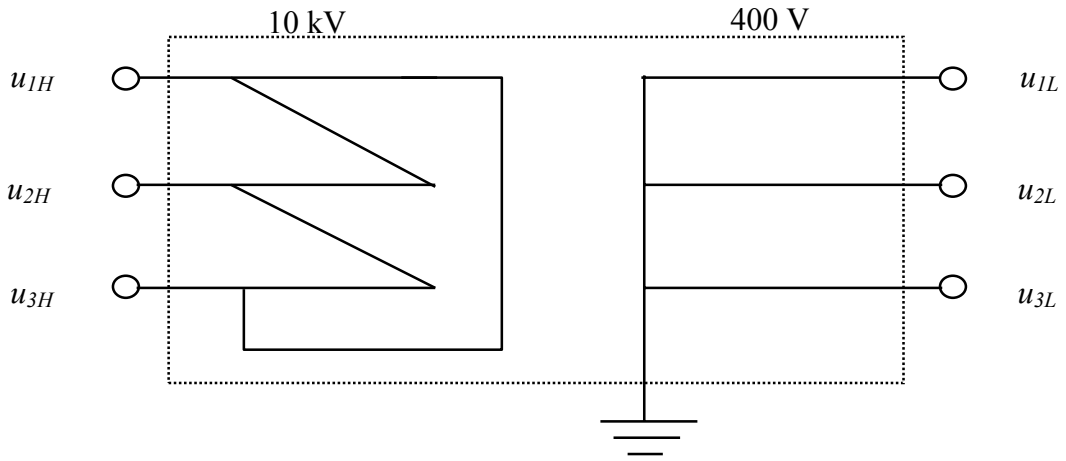

Fig. 8. Delta-star transformer

C.4.1 Zero-crossing capacitor energising

Fig. 9 shows the phase-to-ground voltages that are measured at the lower voltage side of a delta-star transformer during zero-crossing capacitor energising that takes place at the high voltage side and the corresponding LWL of them. The waveforms were obtained from an EMTP simulation. Fig. 10 shows the phase-to phase voltages and the corresponding LWL.

The maxima of LWL of all phase-to-phase voltages are at zero crossings and the time difference between them is equal to the time difference between the switching of the different phases (3.33 msec). As (2) shows, each one of the phase-to-phase voltages corresponds to a phase-to-ground voltage at the higher voltage side, and it is the transient of this voltage that is detected using the DWT. So, the phase-to-phase voltages should be used for classification purposes.

It must be highlighted here that the total transient for the whole switching sequence is different for each phase. The system before the first phase is switched is symmetrical, but this is not true during the switching procedure. The system returns back to symmetry only after the third phase is switched.

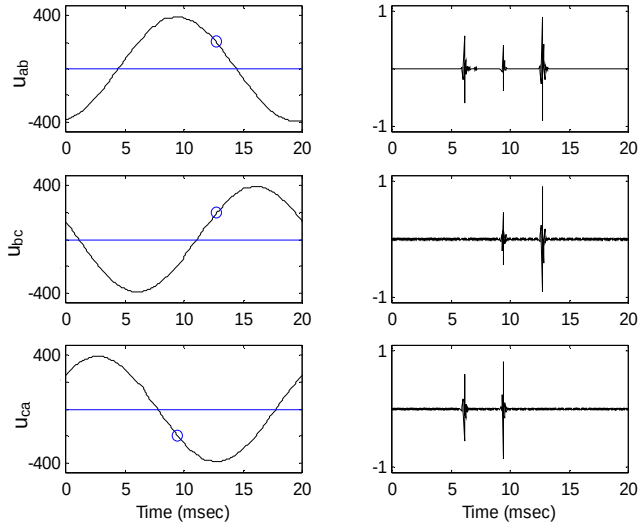

Fig. 9. (left) Phase-to-ground voltages during zero-crossing capacitor energising (EMTP simulation) (right) LWL

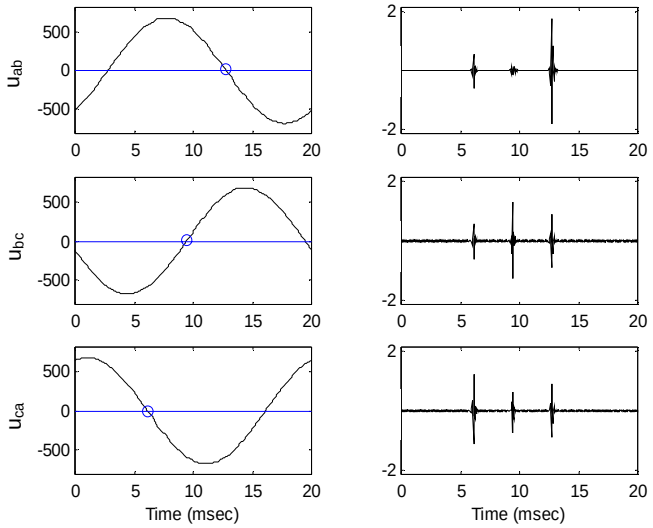

Fig. 10. (left) Phase-to-phase voltages during zero-crossing capacitor energising (EMTP simulation) (right) LWL

C.4.2 “5 msec”-capacitor energising

The phase-to-ground voltages that are measured on the low voltage side of a delta-star transformer when “5 msec”-capacitor energising takes place in the high voltage side are similar to the phase-to-phase voltages used before, when measurements are available from the voltage level where the switching takes place. Therefore, the following can be expected:

1. that one phase has only one major transient, and this is the one that corresponds to the simultaneous switching of the two phases (step 1).
2. that one phase-to-phase voltage has only one major transient that corresponds to the switching of the third phase. By (2), subtracting the measured phase-to-ground voltages,

sums of the phase-to-ground voltages of the high voltage side are created. So, a transient due to step 1 will not be present in one of the phase-to-phase voltages (step 1 causes anti-symmetric transients in two of the phases and their sum is almost zero).

Fig. 11 shows the measured phase-to-ground voltage waveforms during "5 msec"-capacitor energising and the corresponding LWL of them. The switching took place at the 10 kV side of a delta-star transformer and the monitor was connected in the low voltage (400 V) system. The voltage waveforms are distorted due to harmonics. However, the DWT is able to detect the transient that is due to the switching. Using LWL a transient is detected close to the zero-crossing of phase-b voltage. Fig. 12 shows the phase-to-phase voltages. As expected the difference of phase-a and phase-c voltages has a major transient 5 msec after. So, for classification purposes, the maximum of the LWL of one of the phase-to-phase voltages (u_{ca} in Fig. 12) must be close to zero and the maximum of the LWL of the remaining phase-to-ground voltage (u_b in Fig. 11) 5 msec (90°) before.

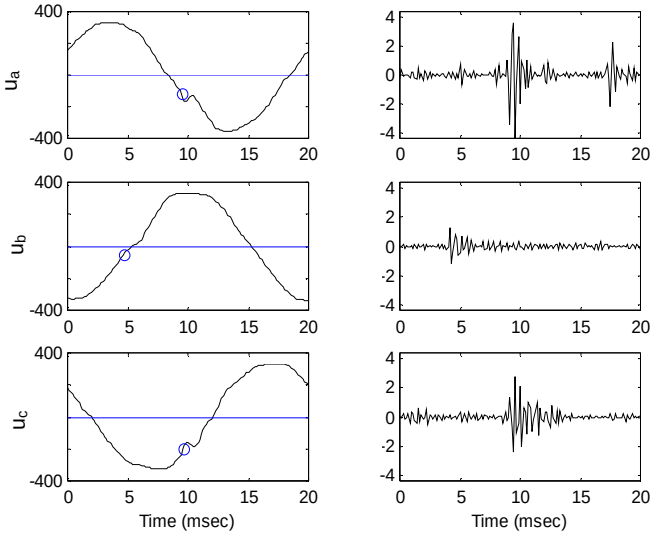

Fig. 11. (left) Phase-to-ground voltages during "5 msec"-capacitor energising (measurement) (right) LWL

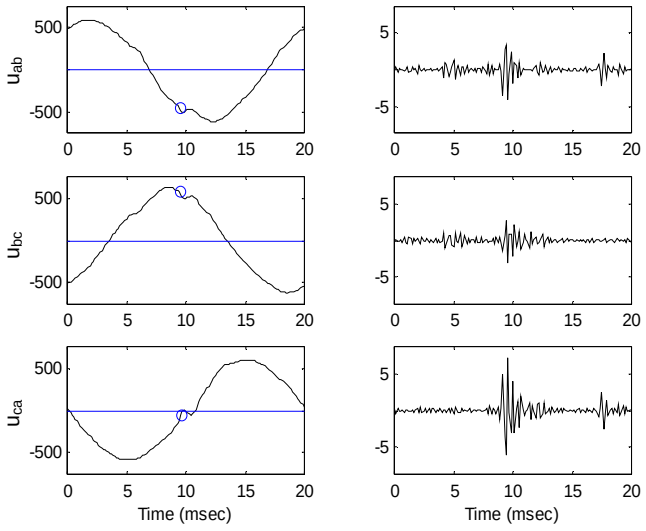

Fig. 12. (left) Phase-to-phase voltages during "5 msec"-capacitor energising (measurement) (right) LWL

C.5. Classification algorithm

The results of the above analysis are summarised in Fig. 13. The detection procedure should be applied to both phase-to-ground and phase-to-phase voltages. A set of rules utilises the outcome of the detection procedure and all the cases that were described above can be classified. As mentioned already, there are certain points on the wave that the classification algorithm considers. However, as measurements showed, the switching might deviate from these points, and the classification algorithm should take this into account by allowing small deviations around them.

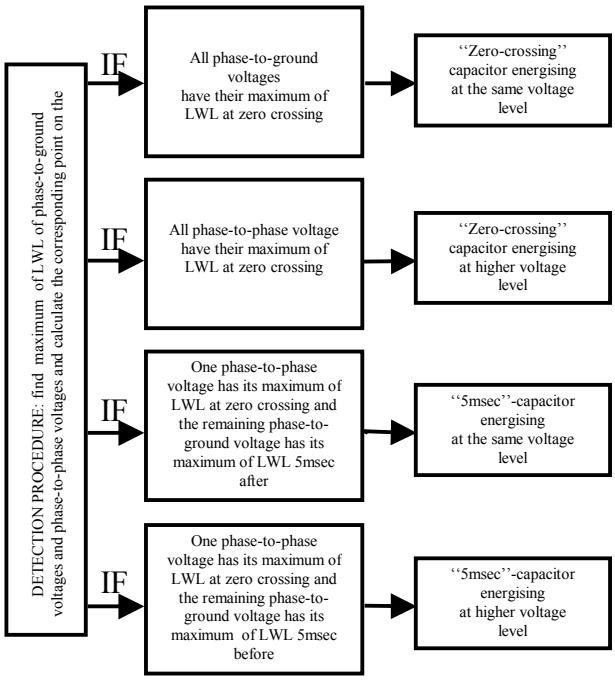

Fig. 13. The structure of the classification algorithm

C.6. Amplification of harmonic distortion due to capacitor energising

Capacitor switching might lead to amplification of harmonic distortion due to resonance that is created by the addition of the capacitor [8]. Such a situation must be identified, because the measured harmonics do not accurately represent the polluting loads. Especially when harmonic distortion exceeds the specified limits, actions should be taken that could include the installation of filters.

Fig. 14 shows the harmonics of phase-a voltage one cycle before and one cycle after the capacitor switching (the actual waveform is given in Fig. 6). The total harmonic distortion (THD) in voltage was increased (from 0.61% to 0.95%) mainly due to the increase of the 5^{th} harmonic. Fig. 15 shows the harmonics of phase-a current, one cycle before and one cycle after the capacitor switching (the actual waveform is given in Fig. 6). The total harmonic distortion (THD) in current was increased (from 1.28% to 2.8%). By classifying the switching event (as capacitor energising) it became evident that the increase in the harmonic distortion was not due to a load but due to the amplification phenomenon.

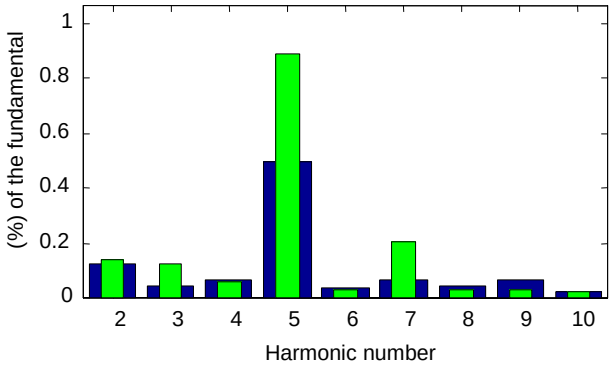

Fig. 14. Voltage harmonics (phase-a) before the switching (wide bar) and after (narrow bar) (data provided by GENAB)

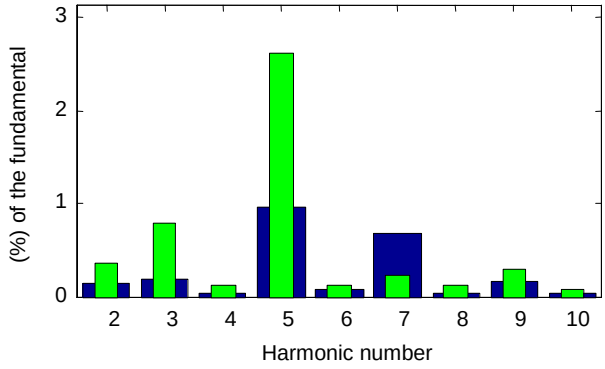

Fig. 15. Current harmonics (phase-a) before the switching (wide bar) and after (narrow bar) (data provided by GENAB)

C.7 Conclusions

This paper presents a new algorithm for classification of transients due to synchronised switching. Zero-crossing and "5 msec"-capacitor energising are considered. The special features of each case are presented and analysed using measurements and simulations.

The classification is based on the extraction of the point on the wave on the phase-to-ground voltage waveforms where the switching of each phase takes place. DWT is utilised for this purpose. In the simulations, the maximum of LWL of each phase corresponds to the switching of this phase. However, the measurements showed that a small change in the switching instants causes a transient that is the largest for all phases. To overcome this problem, the phase-to-phase voltages are utilised and the results show that classification is possible. The same approach is extended to the case that the produced transients propagate in the system through delta-star transformers.

For the classification of zero-crossing capacitor energising: the maximum of the LWL of all the phase-to-ground voltages must close to zero crossing (if the switching takes place at the same voltage level), or the maxima of the LWL of all the phase-to-phase voltages must be at zero (if the switching takes place at higher voltage level and the transients

propagate through a delta-star transformer). The time difference between two consecutive maximums should be 3.33 msec (50 Hz system). Only simulations are used for the zero-crossing capacitor energising case and measurements are needed to verify the simulations. In the case that the switching of one phase produces a transient into the other two phases that has larger amplitude than the one produced by their switching then a more complicated detection approach should be employed. It will detect three peaks at each phase, equally spaced in time, for all phase-to-phase voltages.

For the classification of "5 msec"-capacitor energising: the maximum of the LWL of one of the phase-to-phase voltages must be close to zero and the maximum of the LWL of the remaining phase-to-ground voltage 5 msec after (if the switching takes place at the same voltage level) or 5 msec before (if the switching takes place at higher voltage level and the transients propagate through a delta-star transformer). Both simulations and measurements were used to test the classification algorithm. The synchronised switching classification method enables faster analysis of the data obtained from a power quality survey. Additionally, it can be used to identify problems related to capacitor switching, like amplification of harmonic distortion due to resonance.

C.8. References

[1] M. Kezunovic, I. Rikalo: Automating the analysis of faults and power quality, IEEE Computer Applications in Power, vol. 12, no. 1, January 1999, pp. 46 –50.

[2] P.P. Barker, J.J. Burke, R.T. Mancao, T.A. Short, C.A. Warren, C.W. Burns, J.J. Siewierski: Power quality monitoring of a distribution system, IEEE Transactions on Power Delivery, vol. 9, no. 2, April 1994, pp. 1136 –1142.

[3] V.E. Wagner, J.P. Staniak, T.L. Orloff: Utility capacitor switching and adjustable-speed drives, IEEE Transactions on Industry Applications, vol. 27, no. 4, July-August 1991, pp. 645 –651.

[4] E.P. Dick, D. Fischer, R. Marttila, C. Mulkins: Point-on-wave capacitor switching and adjustable speed drives, IEEE Transactions on Power Delivery, vol. 11, no. 3, July 1996, pp. 1367 –1372.

[5] R. Soderstrom, L. Liljestrand, L. Paulsson: Fast and soft switching of capacitor banks, CIRED, 13th International Conference on Electricity Distribution, Liege, Belgium, 1995.

[6] G. Strang, T. Nguyen: Wavelets and Filter Banks, Wellesley-Cambridge Press 1996.

[7] I.Y.H. Gu, M.H.J. Bollen: Time-Frequency and Time-Scale domain analysis of voltage disturbances, to appear in IEEE Transactions on Power Delivery 2000.

[8] A.A. Girgis, C.M. Fallon, J.C.P. Rubino, R.C. Catoe: Harmonics and transient overvoltages due to capacitor switching, IEEE Transactions on Industry Applications, vol. 29, no. 6, November-December 1993, pp. 1184 –1188.

Paper D Transformer saturation after a voltage dip

Abstract

This paper reports on a new type of power system event that was observed during a monitoring program. According to measurements at different voltage levels, transformer saturation might occur due to the voltage recovery after a voltage dip. This type of event has not been presented before in the literature. Measurements of current and voltage are presented and analysed in terms of harmonic distortion.

Keywords

Power system measurements, transformer saturation, fault clearing, harmonic distortion, power quality, voltage dip.

D.1 Introduction

The increasing importance of power quality forces power utilities to run monitoring programs in their networks. The output of these programs is not only used to improve the quality that is offered to the customers but also extends our knowledge in power system operation. New phenomena are observed that had not been reported and taken into account before.

Transformer saturation is due to the sudden energising of the magnetising flux. If the energising takes place at an appropriate place of the voltage sinewave, the flux (being the integral of the voltage) contains a dc component which may take long time to decay. Transformer saturation especially occurs for non-loaded or lightly loaded transformers. However, a transformer might saturate in occasions other than energising. One case is the phenomenon of sympathetic interaction between transformers, which is likely to occur when a transformer is energised from a system to which there are other transformers already connected. The inrush current makes the voltage at the point of common coupling asymmetrical. As the flux in a transformer is strictly proportional to the area (integral) of the voltage waveform, the flux in the already connected transformers becomes asymmetrical, producing an offset flux that drives these transformers to saturation [1]. One more case is presented in [2]. The circulation of direct current in transformer windings due to static var-compensators with anti-parallel thyristor arrangement can cause significant saturation and harmonic generation. The DC flux generated by the DC current offsets the alternating flux in the transformer iron core, causing the so-called half cycle saturation.

In this paper we present a new case of transformer saturation. Measurements showed that transformer saturation might occur after a voltage dip. A short-circuit fault occurred in the 400 kV transmission system in Sweden, on 12 October 1999, at 00:30 in the morning, leading to a voltage dip for all customers in Gothenburg and surroundings. The voltage dip has been measured at 132 kV, 10 kV and 400 V voltage levels. In the analysis of the

phenomenon special attention is given to the harmonic contents of voltage and current.

D.2 Measurements

Fig. 1 shows voltages as measured in the 132 kV network. Around 150 msec a voltage dip occurs. From a comparison with the results of a theoretical analysis it was concluded that the cause of this dip was probably a two-phase-to-ground fault. Phase-b and c experience a voltage dip that lasts approximately 5 cycles. The dip in phase-a is shallower. When the protection system operates to clear the fault, the voltage recovers to its pre-fault value. However, a second voltage dip occurs 400 msec later following the reclosing operation because the fault was not removed. The protection system operates again and the voltage recovers.

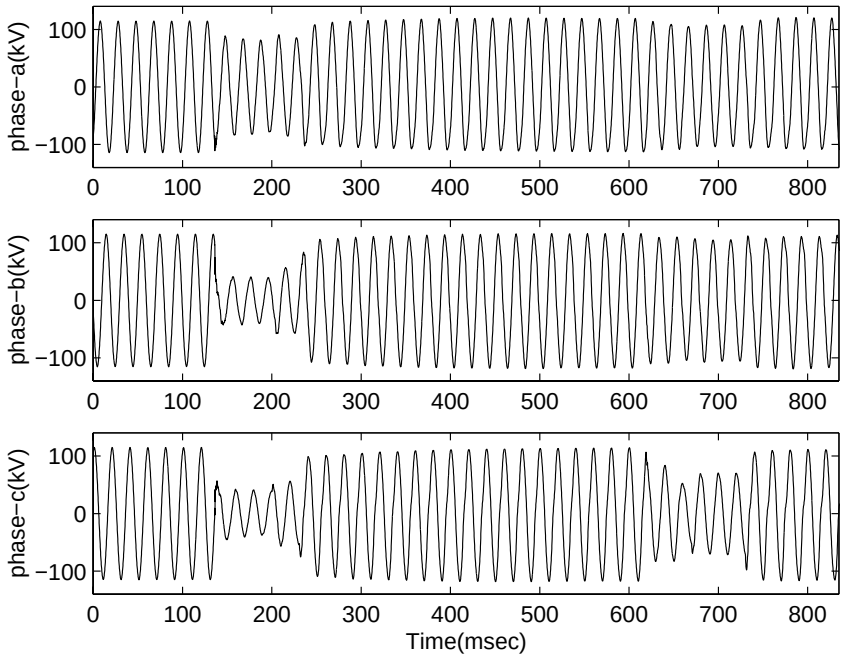

Fig. 1. Voltages before, during and after the voltage dip.

Fig. 2 shows the fundamental voltage magnitude obtained by the Short Time Fourier Transform (STFT), using a sliding window of one cycle [3]. These plots reveal that voltage recovery following the first dip is not immediate. After the fault clearing operation that causes a step increase, all the phases experience a prolonged voltage dip that recovers gradually. It can be seen that there is a small unbalance between the magnitude of the voltages during this stage. A similar phenomenon is mentioned in [4], where the post-fault voltage dip is due to the induction motor re-acceleration. But in this case the post-fault voltages are balanced. Fig. 3 shows the currents of phase-a and c. (Phase-b current is not available). During the first voltage dip these currents increase in magnitude. During the fault clearing operation and at the same instant that voltage starts recovering, phase-c current becomes very distorted. After fault clearing the current waveforms show high distortion that decays slowly; the main characteristic of this distortion is the asymmetry between the positive and the negative half cycle. After the

second dip the distortion in current increases. The harmonic analysis that is presented in the following section shows high even harmonics in both voltage and current. These characteristics are indicative of transformer saturation. The high magnetising current following the fault clearing operation explains the prolonged voltage dip that recovers gradually (Fig. 2). The difference in the magnitude of the voltage dip between the phases is due to the different degrees of saturation of each phase.

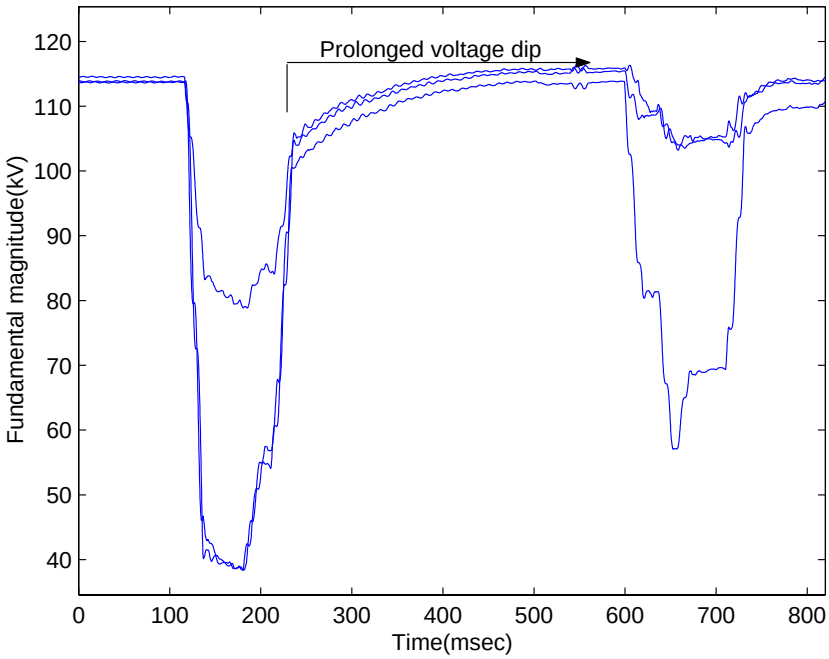

Fig. 2. Fundamental voltage magnitude as a function of time for the voltages shown in Fig.1.

D.3 Harmonic analysis

Even harmonics (2^{nd}, 4^{th}, etc) are the characteristic harmonics of transformer saturation and they are used to restrain the operation of the differential protection of the transformer during energising. Even harmonics are not common in power systems and basically depict the asymmetry between the positive and negative half cycle of the waveform. Fig. 4a shows the amplitude of the 2^{nd} harmonic of phase-a voltage in time using the STFT (all harmonics are plotted as percentage of the pre-fault fundamental voltage and current). There is no significant 2^{nd} harmonic before the first voltage dip. The first peak is due to the step decrease in voltage following the fault initiation. Two more peaks are present during the voltage dip but before fault clearing no sustained 2^{nd} harmonic component is observed. However, after the fault clearing, the 2^{nd} harmonic distortion increases to approximately 7% of the pre-fault fundamental voltage and then decays slowly. Similar behaviour is seen in the amplitude of the 2^{nd} harmonic of phase-a current (Fig. 4b). There is a temporary increase during the voltage dip, and the 2^{nd} harmonic component becomes significant after the fault clearing. It reaches a maximum value of approximately 20% of the pre-fault fundamental current and then it decays slowly in the same manner as the voltage. Similar results were obtained for the other phases. The harmonic distortion sustains after the second voltage dip. Fig. 4 shows that the second harmonic becomes even higher after the second protection operation.

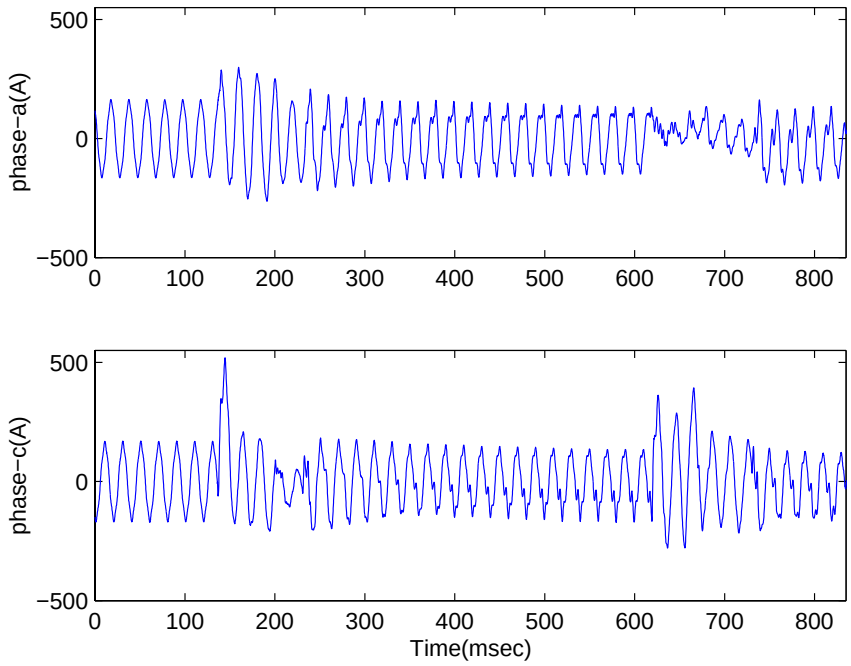

Fig. 3. Currents before, during and after the voltage dip.

The harmonic analysis showed also that the 3rd and 4th harmonic components of voltage and current after the fault clearing are high. However, the 2nd harmonic component is the dominant one. These results are consistent with the results that have been presented in the literature for transformer saturation cases, like in [1]. The presence of the even harmonics and their decaying nature are typical for transformer saturation.

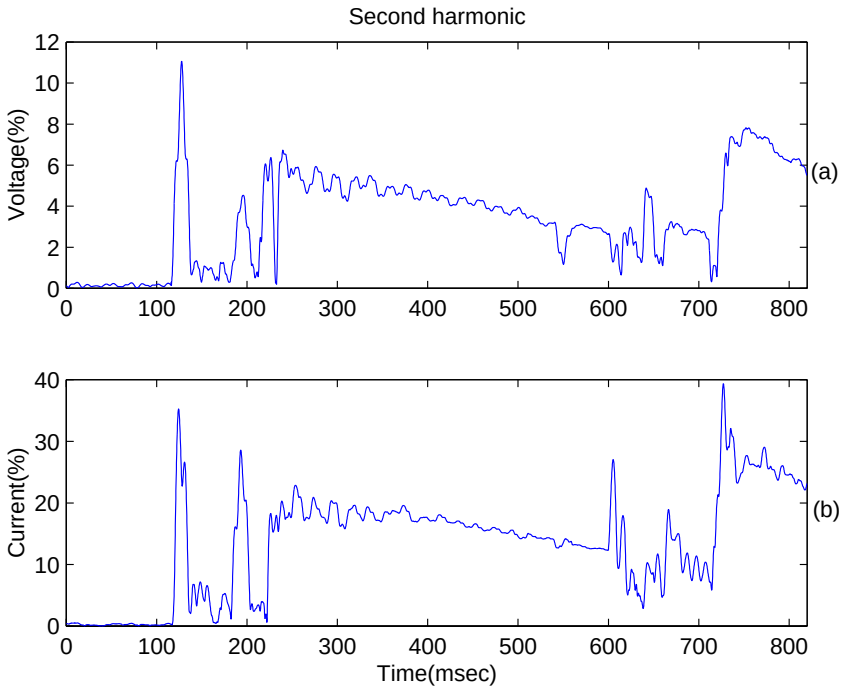

Fig. 4. (a) 2nd harmonic of phase-a voltage (b) 2nd harmonic of phase-a current.

D.4 Discussion -Conclusions

It is shown here that voltage recovery after a fault may lead to transformer saturation. Both the voltage and the current distortion show the behaviour typical of transformer saturation. The cause of transformer saturation after a voltage dip is the same as after energising: a sudden change in voltage leads to a dc component in the magnetising flux. As the voltage dip is short, remanent magnetism may aggravate the phenomenon. Also note that the voltage dip occurred at night so that it is likely that some 10kV/400V transformers have been lightly loaded. These transformers will go into saturation on voltage recovery, leading to a heavily distorted current at 10 kV and higher voltage levels. The current measured at 10 kV showed a large distortion, like the current at 132 kV. The distortion of the current at 400 V was small. Further data analysis and simulation is needed to quantitatively explain the phenomenon.

The same phenomenon has been observed in more measurements. Fig. 5 shows the voltage waveforms during a voltage dip due to a fault. The fault is removed in less than half a cycle, probably due to a fuse operation. It can be seen that the voltage waveforms are distorted after the voltage recovery. Fig. 6 shows the fundamental voltage magnitude of measurements. Phase-b that experiences the fault recovers gradually after fault clearing. The harmonic analysis gives similar results as in the case that is presented in Fig. 4.

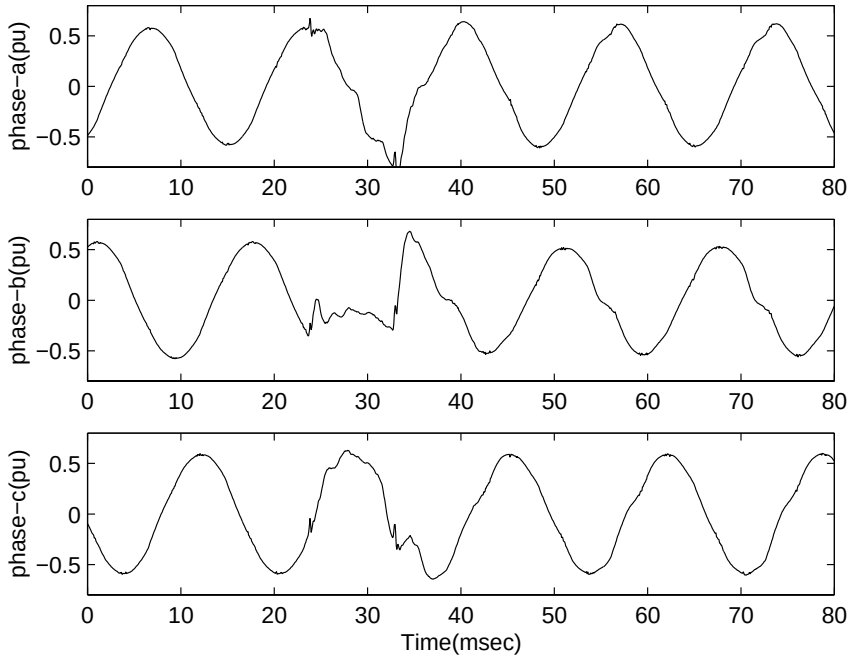

Fig.5. Voltages during a voltage dip that causes transformer saturation

A similar phenomenon is described next: Fig. 7 shows the voltage waveforms during a fault followed by a reclosing in a medium voltage system. The fundamental frequency magnitude (Fig. 8) shows that the reclosing causes a voltage dip for all three phases of different magnitude for each phase that recovers gradually. Fig. 9 shows the currents during the reclosing. The distortion is obvious in all phases, and its main characteristic is

the asymmetry between the positive and the negative half cycle. Harmonic analysis showed that after the reclosing, the harmonic distortion increases significantly similarly to Fig. 4, and the even harmonics are dominant.

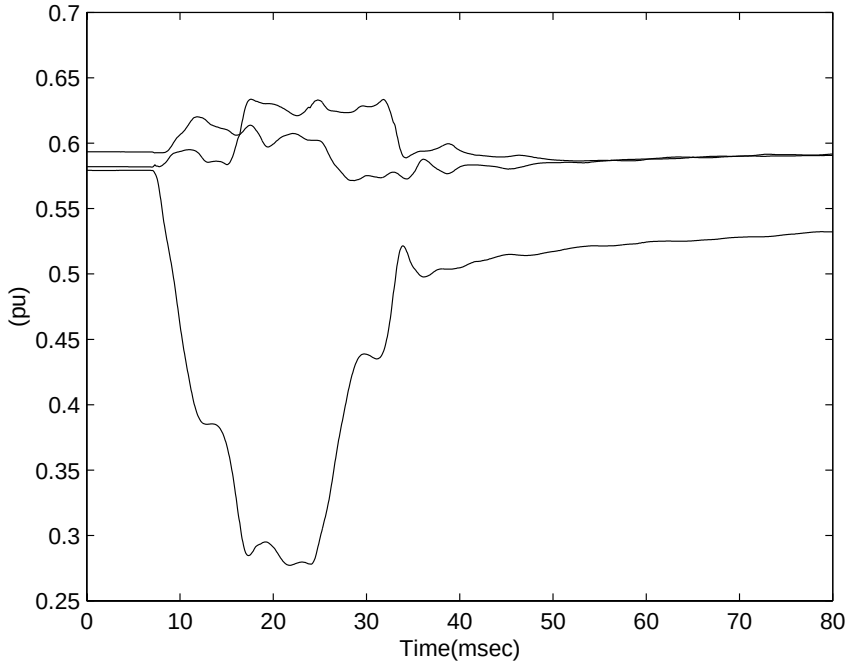

Fig. 6. Fundamental voltage magnitude as a function of time for the voltages shown in Fig.5

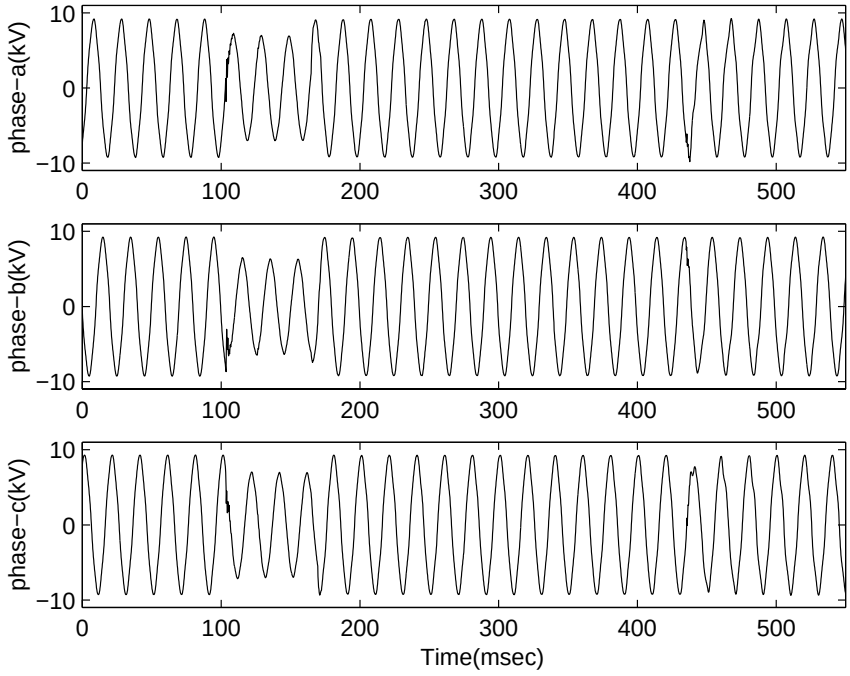

Fig.7. Voltages during a voltage dip followed by a reclosing

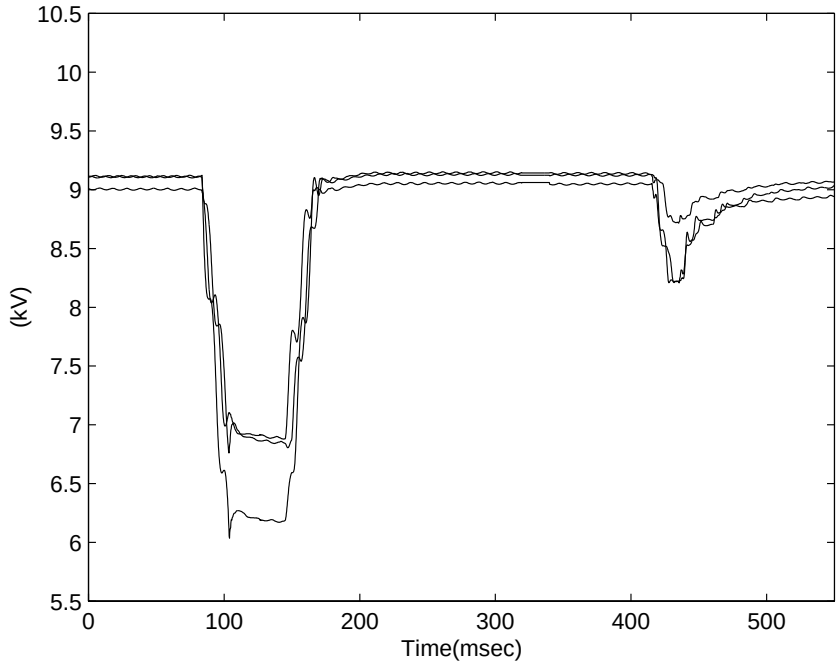

Fig. 8. Fundamental voltage magnitude as a function of time for the voltages shown in Fig.7

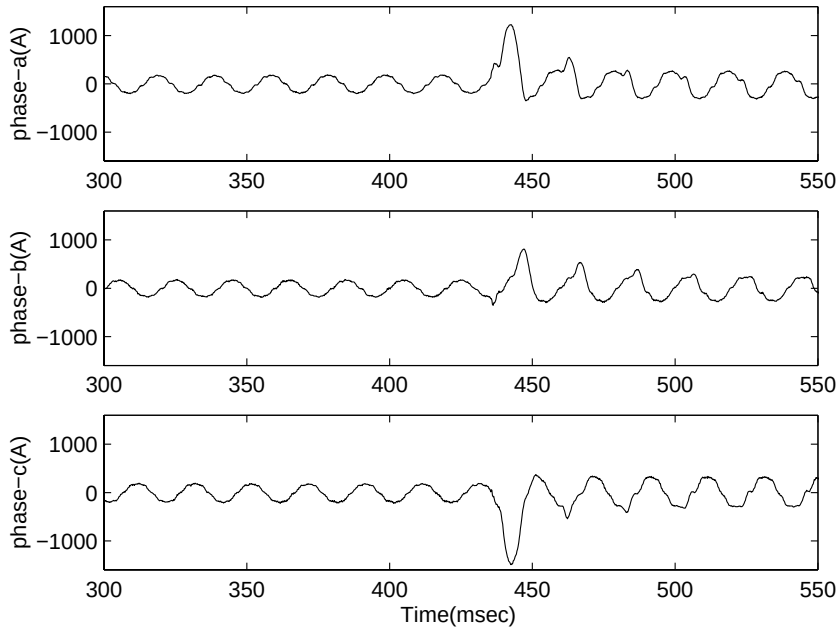

Fig. 9. Current waveforms during reclosing

Transformer saturation has not received attention other than the one relevant to energising and its effect on differential protection, and it has been a concern mainly for non-loaded transformers. The above measurements show that saturation may occur even for transformers that are loaded: after a voltage dip; either immediately after the dip or during the reclosing operation. The effects of this phenomenon are temporarily increased harmonic distortion and prolonged voltage dips. Further data analysis and simulations are

needed to quantitatively explain the phenomenon.

D.5 References

[1] H.S. Bronzeado, P.B. Brogan, R. Yakamini: Harmonic analysis of transient currents during sympathetic interaction, IEEE Transactions on Power Delivery, vol. 11, no. 4, November 1996, pp. 2051-2056.

[2] W. Xu, T.G. Martinich, J.H. Sawada, Y. Mansour: Harmonics from SVC transformer saturation with direct current offset, IEEE Transactions on Power Delivery, vol. 9, no. 3, July 1994, pp. 1502-1508.

[3] I.Y.H. Gu, M.H.J. Bollen: Time-Frequency and Time-Scale domain analysis of voltage disturbances, to appear in IEEE Transactions on Power Delivery 2000.

[4] M.H.J. Bollen: The influence of motor re-acceleration on voltage sags, IEEE Transactions on Industry Applications, vol. 31, no. 4, July-August 1995, pp. 667 –674.

Paper E — Classification of power system events: Voltage dips

Abstract

The extensive monitoring programs that are run by power utilities enable new insights of the power system operation and new characterisation methods must be used for the classification and analysis of the recordings. This paper focuses on events that cause a temporary decrease in the fundamental frequency voltage magnitude (voltage dip). The analysis of the recordings from surveys in medium and low voltage networks shows that new classes of voltage dips should be introduced in order to characterise the events that are captured by the power quality monitors. The aim of the paper is to show the distinctive characteristics of each class and give the guidelines for the automatic processing of the recordings. Finally, a large number of recordings from a medium voltage network are classified using these characteristics and the results are presented.

Keywords

Power system monitoring, power quality, voltage dips, power system faults, power transformers, induction motors, short time Fourier transform.

E.1 Introduction

The importance of power quality in the operation and design of power systems is widely accepted. Utilities are forced to prove that the offered power meets the specified standards and the requirements of the customers. Furthermore, when the quality of power is not accordant with these requirements, immediate action should be taken. For these reasons power utilities run extensive monitoring programs in order to provide statistics regarding the quality of the power and the necessary information for the solution of problems. Additional benefit of monitoring is that the engineers obtain new knowledge about system operation. The developments in communications and electronics make monitoring even more attractive from a cost point of view, and it is expected that more monitors will be installed in the coming years.

According to their settings, the monitors capture different types of events, and long sequences of measurements are transferred to the databases. Some of these events are due to normal system operations, do not cause any problem and are not of particular interest, while others need to be categorised according to the needs of the monitoring program. When an event presents characteristics that cause or might cause problems, then the system must give an alarm. Because of the large size of these databases, new tools are required that will enable the automatic processing of the recordings.

This paper focuses on a large class of power system events: the main characteristic of these is a temporary decrease in the fundamental frequency voltage (voltage dip) in one or more phases. Voltage dips have attracted a lot of attention due to the problems that cause to equipment like adjustable speed drives, computers, industrial control systems etc.

They are mainly caused by faults and induction motor starting [1-2].

It has been clarified already that voltage dips cannot be characterised by a single magnitude and duration for each phase. In [3], it is shown that these values are inadequate in describing a voltage dip, and especially its impact on sensitive loads. In [4], the case in which the voltage dip contains multiple components is highlighted.

The aim of this paper is to show that there are certain types of voltage dips that should be considered in the analysis of monitoring data as showed the analysis of a large number of recordings. Furthermore, the distinctive characteristics of each type are extracted and presented. For the analysis of the different types of voltage dips, recordings are used that were performed at medium and low voltage networks in Sweden (by Göteborg Energi Nät AB-GENAB), Norway (by the Norwegian Electric Power Research Institute-SINTEF) and Scotland (by Scottish Power). Finally, a large set of recordings is classified, explained and presented in terms of the above mentioned types.

E.2 Background

E.2.1 Short Time Fourier Transform.

The squared magnitude of the Fourier Transform is the classic method used to represent the frequency domain information (spectrum) of a stationary signal. However, this approach does not provide any information on the time properties on the frequency components that the signal contains. The Short Time Fourier Transform (STFT) overcomes the problem by partitioning the signal into short time segments (during which the signal is considered stationary) then applying a weighting function to the signal within each segment, prior to evaluating the Fourier Transform. This provides a time-frequency distribution of the signal which represents the evolution of the signal spectrum as a function of time. Let $x(n)$ represent a discrete time signal, the STFT at time $n\Delta t$ and frequency f is defined as [5]:

$$Xs(n,f) = \sum_{m=-\infty}^{+\infty} w(n-m)x(m)e^{-j2\pi fm} \qquad (1)$$

where w is the analysis window that selectively determines the portion of $x(n)$ for analysis. In this paper STFT is used to extract the fundamental frequency of voltage and its harmonics. For the purposes of this paper, the STFT was applied using a rectangular weighting window and the segmentation of the analysed signals was in overlapping blocks of one cycle.

E.2.2 Voltage dips due to faults

Voltage dips due to faults can be severe and therefore are of major concern. They cause problems to a large number of customers as they propagate in the system. The magnitude of this type of voltage dip at a certain point in the system depends mainly on the type of the fault, the distance to the fault, the system configuration and the fault resistance. Its

duration depends on the type of protection that is used, and varies between half a cycle (for a fuse) to a few seconds. [2]. Faults are either symmetrical (three phase or three phase-to-ground faults) or non-symmetrical (single phase or double phase or double phase-to-ground faults). Depending on the type of fault, the magnitudes of the voltage dips of each phase might be equal (symmetrical fault) or unequal (non-symmetrical faults). Fig. 1 shows the voltage waveforms during a fault-induced voltage dip. The measurement was performed in an 11 kV network. The duration of the dip is approximately 5 cycles, which is the typical time for a circuit breaker to open after it receives a trip command from the system's protection relays. The recovery of voltage is fast and it creates an almost rectangular shape for the fundamental frequency voltage magnitude.

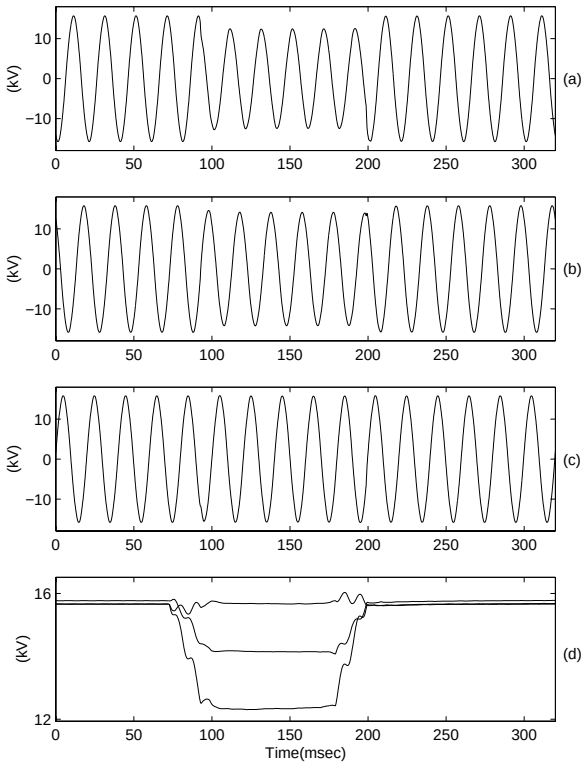

Fig.1. (a)-(c) Phase-to-phases voltage waveforms during a fault (d) The fundamental frequency magnitude of voltage

E.2.3 Voltage dips due to induction motor starting

During starting, motors draw approximately five-times their full-load running current at a very low power factor. This starting current causes shallow voltage dips. The magnitude of the voltage dip depends on the characteristics of the induction motor and the strength of the system at the point that the motor is connected.

Fig. 2 shows the voltage waveforms during a voltage dip due to induction motor starting. The measurement was performed in a 400 V network. The fundamental frequency voltage magnitude of all phases drops approximately 10% of the pre-event value and then recovers gradually as the current that is drawn by the motor decreases.

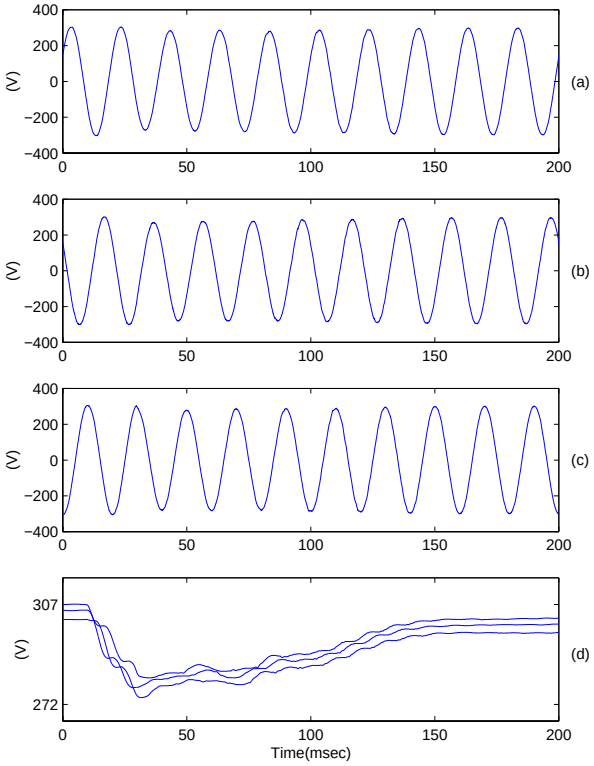

Fig.2. (a)-(c) Phase-to-ground voltage waveforms during induction motor starting (d) The fundamental frequency magnitude of voltage

E.3 Other voltage dip types

E.3.1 Multistage voltage dips

Multistage voltage dips are due to faults, but they present different levels of magnitude before the voltage returns back to normal. Fig. 3 shows the voltage waveforms during a multistage voltage dip. The measurement was performed in an 11 kV network. As the fundamental frequency magnitude of voltage shows, the voltage dip magnitude shows an additional step before the final voltage recovery. These steps in the voltage dip magnitude can be due either to changes in the system configuration while the protection system tries to isolate the fault, or changes in the nature of the fault itself. A typical situation is a fault in the transmission system that is not cleared during the operation of zone 1 distance protection but only during the zone 2 operation. An example is given next.

Consider as an example the subtransmission loop of Fig. 4. Suppose that Z_1 and Z_2 are the impedances between the source and the load bus, Z_0 the source impedance and that a fault occurs between the circuit breakers CB1 and CB2 at fraction p from the source. The voltage dip at the load bus (in p.u.) is given by [6]:

$$V_{dip1} = \frac{p(1-p)Z_1^2}{Z_0(Z_1+Z_2)+pZ_1Z_2+p(1-p)Z_1^2} \qquad (2)$$

If CB1 opens to clear the fault then the load bus will experience a voltage dip of

magnitude:

$$V_{dip2} = \frac{(1-p)Z_1}{Z_0 + Z_2 + (1-p)Z_1} \qquad (3)$$

By comparing the denominators of the above formulas it is easy to see that the opening of CB1 will lead to an increase in voltage (because: $Z_0(Z_1+Z_2)>pZ_0Z_1$). The voltage dip at the load bus will recover completely only after circuit breaker CB2 opens.

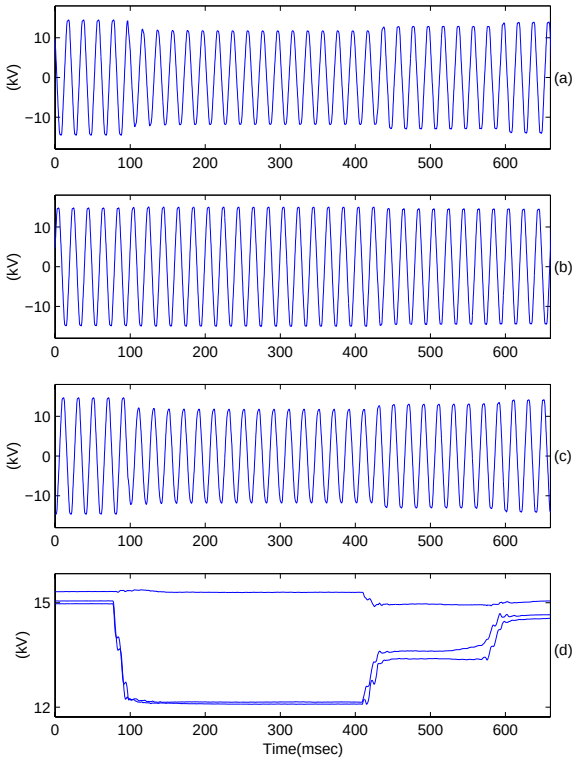

Fig.3. (a)-(c) Phase-to-phase voltage waveforms during a fault (d) The fundamental frequency magnitude of voltage

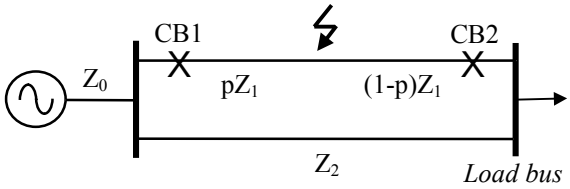

Fig.4. Equivalent circuit for faults in a subtransmission loop

E.3.2 Voltage dips due to self-extinguishing faults

Voltage dips due to self-extinguishing faults are the ones that disappear before the fastest possible breaker opening time. Fig. 5 shows the voltage waveforms during a self-

extinguishing voltage dip. The measurement was performed in a 10 kV network. As the fundamental frequency magnitude of voltage shows, the voltage decreases for less than 2 cycles before it disappears without causing operation of the protection system.

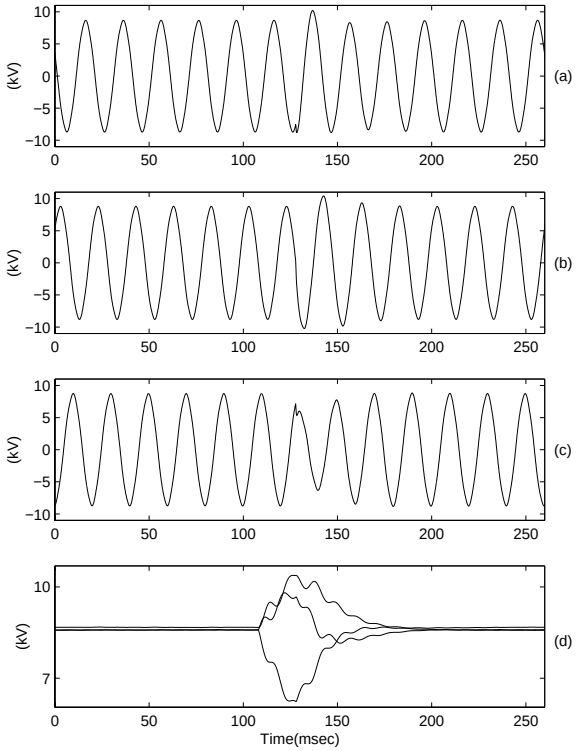

Fig.5. (a)-(c) Phase-to-ground voltage waveforms during a self-extinguishing fault (d) The fundamental frequency magnitude of voltage

E.3.3 Voltage dips due to transformer energising

Voltage dips due to transformer energising have been reported in the literature [7], but neither the frequency in which this event appears in a power quality survey nor the characteristics of this event in terms of voltage have been presented. The main attention has been given to the effects of the inrush current on the protection relays of the transformer itself [8]. In a transformer under steady-state conditions, there is a particular value of flux in the core, for each point on the voltage waveform. When the transformer is energised, the initial value of flux in the core might not necessarily be the steady-state value for this particular point on the voltage waveform. A transient will occur to change the flux in the core to the steady state condition. In general this will cause the flux to go above the saturation value once each cycle until the average value of the flux for a cycle has decayed to nearly zero. This temporary over-fluxing of the transformer core causes high values of the magnetising current.

This phenomenon is known as magnetising inrush current. In turn, short duration voltage dips are caused that might result in an unwanted tripping of differential protective relays. As described in [7] and [9] this voltage dip can be long in duration and drive more

transformers into saturation. The phenomenon is called sympathetic interaction.

Fig. 6 shows the voltage waveforms during transformer energising. The measurement was performed in an 11 kV network. The fundamental frequency voltage magnitude drops for a very short time and recovers gradually as the magnetising current decreases. The largest drop is approximately 8% of the pre-event voltage.

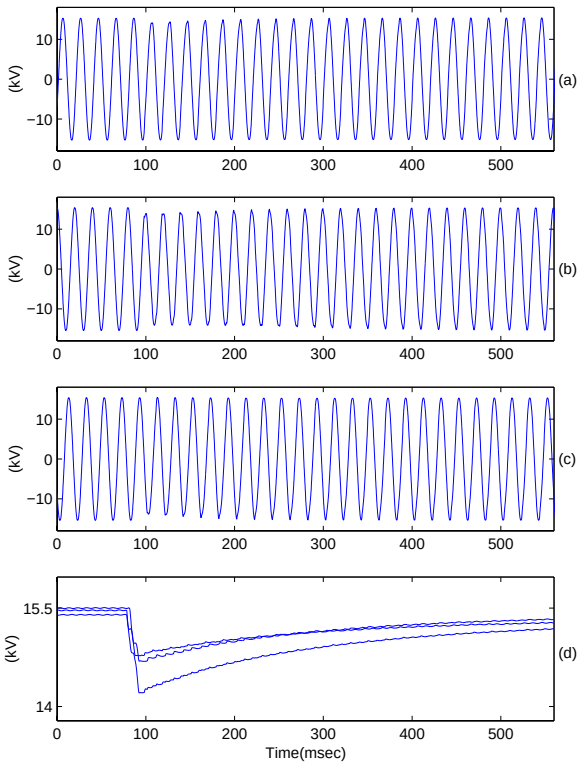

Fig.6. (a)-(c) Phase-to-phase voltage waveforms during transformer energising (d) The fundamental frequency magnitude of voltage

E.4 On the classification of voltage dips

As mentioned in the introduction, automatic processing of the recordings is needed for the analysis of the databases created by power quality surveys. In this direction, the distinctive features of each type must be extracted and utilised in a rule-based system. The analysis of a large number of recordings from different surveys showed that the following characteristics can be used to distinguish between the different types of voltage dips:

The rectangular shape of the fundamental frequency voltage magnitude: voltage dips due to faults have this shape as shown in Fig. 1, due to the operation of protection that clears the fault and forces voltage to recover fast. On the other hand, voltage dips due to induction motor starting and transformer energising recover gradually as show in Fig. 2 and 7, provided that there is no protection maloperation.

The symmetry between the different phases: voltages during induction motor starting are

symmetrical because an induction motor is a balanced load and each phase will draw the same inrush current causing a voltage dip of the same magnitude for all phases as in Fig. 2. In the case of transformer energising this is not true. The inrush current depends on the degree of saturation of each phase. Therefore, each phase will experience a voltage dip of different magnitude (non-symmetrical) as shown in Fig. 6. Finally, voltage dips due to faults can be non-symmetrical as in Fig. 1 or symmetrical as in Fig. 7, depending on the type of the fault.

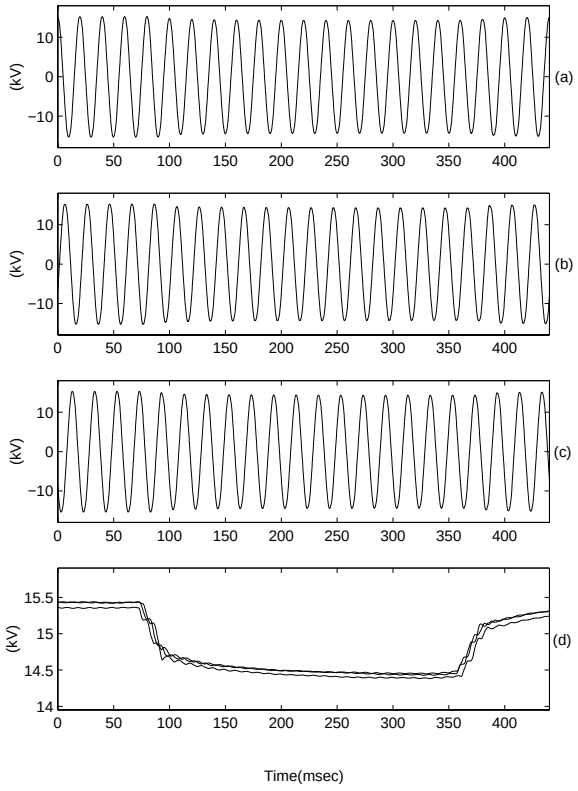

Fig.7. (a)-(c) Phase-to-phase voltage waveforms during a symmetrical fault (d) The fundamental frequency magnitude of voltage

The harmonic contents of voltage during the voltage dip: it is well documented that the voltage waveforms during transformer energising present high harmonic distortion [e.g. 9]. The analysis of voltage waveforms during transformer energising showed that the harmonic distortion is temporary. The even harmonics (second and fourth) are contributing the most as shown in Fig. 8, which shows the harmonics up to the fifth of the first voltage waveform of Fig. 6.

Fig. 9 summarises the features of the different types of voltage dips. These features have already been applied in a ruled-based system for power system event classification and the results show strong potential [10].

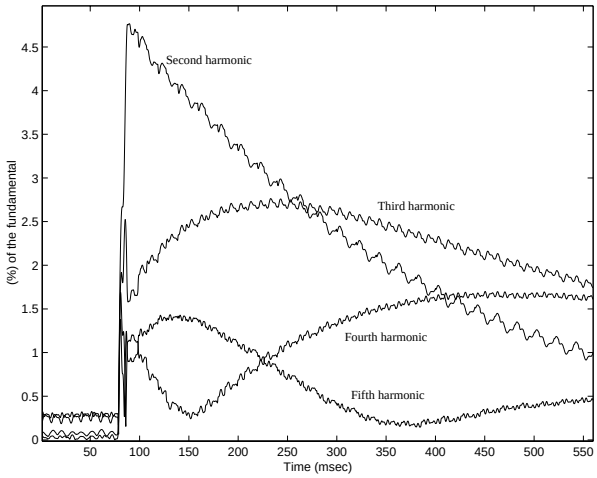

Fig.8. Harmonics of voltage (of Fig. 6) during transformer energising as percentage of the fundamental frequency voltage using the STFT

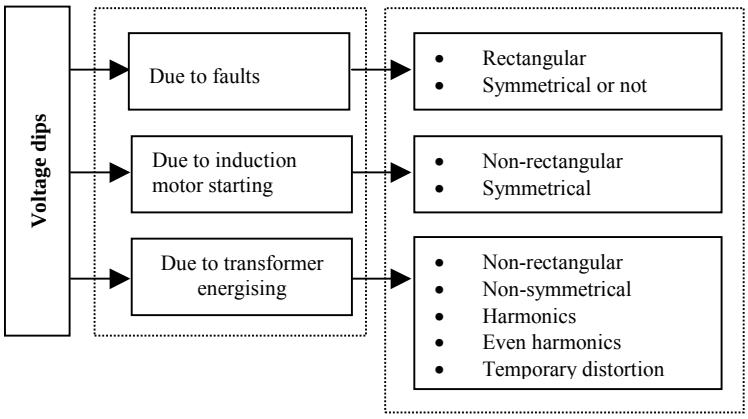

Fig.9. Voltage dip types and their characteristics

E.5 Analysis of a database using the proposed classification

Recordings that correspond to one month of monitoring in a medium voltage network (33 and 11 kV) were analysed using the STFT and using the features that were described in the previous section, the data was classified into different categories as shown in Table 1. Due to an extensive monitoring program in the medium voltage network for several years, a large number of recordings is available. The monitors are triggered by current or voltage disturbances and all the resulting recordings are considered here.

1. Voltage dips due to faults turned out to be the category with the largest number of recordings. They are subdivided into three classes:
a) Voltage dips of duration longer than 3 cycles: this is the largest class of all and their duration varies with the type of protection that is used to clear the fault that caused them.
b) Voltage dips of duration shorter than 3 cycles: these are mainly either due to self-extinguishing faults or fuse-cleared faults. However, it is not clear to the authors for how long a self-extinguishing fault might persist before it disappears. It is possible that self-

extinguishing faults exist in the first subclass (voltage dips longer than 3 cycles). Records of the protection operation from all the voltage levels are needed to accurately extract this type of voltage dip from the database.
c) Multistage voltage dips. In this group there are recordings that have two or even three different levels of voltage dip magnitude. In this category we recognised shallow voltage dips of duration that points towards a fault in the transmission system that is cleared only after zone 2 operation of distance protection.

2. Voltage dips due to transformer energising form a considerable part of the database. These are basically non-rectangular, non-symmetrical voltage dips having a temporary harmonic distortion. This type of event might take place either due to normal system operation (manual energising of a transformer) or due to reclosing actions following the opening of a circuit breaker to clear a fault. There is a possibility that in these recordings the energising of one transformer leads already connected transformers into saturation (sympathetic interaction).

Category 3 contains recordings in which voltage increases or decreases abruptly without a voltage dip. These events could be due to on-load transformer tap changing, capacitor switching or reactor switching. Category 4 consists of recordings that did not present any significant drop in voltage. Most of these recordings were captured by the monitors because of a variation in current. Category 5 contains recordings that although they do contain a voltage dip they could not be explained/classified using the above categories. Voltage dips due to induction motor starting were not found. The explanation is that induction motors connected in low voltage do not cause severe voltage dips in the medium voltage network.

June 1997 Total number of recordings: 756 Number of monitors: 98				
EVENTS-CATEGORIES	1	Voltage dips due to faults	Duration > 3cycles	190 records
			Duration < 3cycles	48 records
			Multistage dips	65 records
	2	Voltage dips due to transformer energising		85 records
	3	Step changes in voltage		134 records
	4	Insignificant drop in voltage		221 records
	5	Unclassified		13 records

Table 1: Classification of the recordings

E.6 Conclusions

The analysis of a large number of recordings mainly from medium voltage networks showed that new characterisation methods are needed because not all voltage dips can be described by a single magnitude and duration for each phase assuming a rectangular shape of the fundamental frequency voltage.

The most interesting findings in the analysed data are:
1. A large part of voltage dips due to faults are multistage, i.e. they present different levels of voltage dip magnitude before the fault is cleared. As explained above this could be either due to a change in the nature of the fault, or due to a change in the system configuration during the protection operation. Further work is needed in order to distinguish between these two cases.
2. A new category of voltage dips should be taken into consideration: those that are due to transformer energising. The number of recordings due to this type of event is significant. This type of voltage dips might take place either due to normal system operation (manual energising of a transformer), or due to reclosing actions following the opening of a circuit breaker to clear a fault.

There is a recognised need for automatic processing of the recordings that are obtained from power quality monitors, because of the large size of the created databases. Towards this direction the distinctive characteristics of the different types of voltage dips are given in section III.

E.7 References

[1] M.H.J. Bollen: Understanding power quality problems: voltage sags and interruptions, New York, IEEE Press, 1999.

[2] Conrad, K. Little, C. Grigg: Predicting and preventing problems associated with remote fault-clearing voltage dips, IEEE Transactions on Industry Applications, vol. 27, no.1, January-February 1991, pp. 167 –172.

[3] M.H.J. Bollen: Characterisation of voltage sags experienced by three-phase adjustable-speed drives, IEEE Transactions on Power Delivery, vol. 12, no. 4, October 1997, pp. 1666-1671.

[4]D.L. Brooks, R.C. Dugan, M. Waclawiak, A. Sundaram: Indices for assessing utility distribution system RMS variation performance, IEEE Transactions on Power Delivery, vol. 13, no. 1, January 1998, pp. 254 –259.

[5]Y.H. Gu and M.H.J. Bollen, Time-frequency and time-scale domain analysis of voltage disturbances, to appear in IEEE Transactions on Power Delivery, 2000.

[6] M.H.J. Bollen: Fast assessment methods for voltage sags in distribution systems, IEEE Transactions on Industry Applications, vol. 32, no. 6, November-December, 1996, pp. 1414–1423.

[7] K.S. Smith, L. Ran, B. Leyman: Analysis of transformer inrush transients in offshore electrical systems, IEE Proceedings in Generation, Transmission, Distribution, vol. 146, no. 1, January 1999, pp. 132-139.

[8] S.H. Horowitz, A.G. Phadke: Power system relaying, Research Studies Press and John

Wiley, Somerset, UK, 1992.

[9] H.S. Bronzeado, P.B. Brogan, R. Yakamini: Harmonic analysis of transient currents during sympathetic interaction, IEEE Transactions on Power Delivery, vol. 11, no. 4, November 1996, pp. 2051-2056.

[10] Varaporn Lawskool: Analysis and automatic classification of voltage dips measured in electric distribution networks, MSc thesis, Chalmers University of Technology, March 2000.